CONF-890310--9
LBL-26298

Center for Advanced Materials

CAM

Presented at the 7th International Conference on Fracture (ICF-7), Houston, TX, March 20–24, 1989, and to be published in the Proceedings

Fatigue-Crack Propagation in Advanced Aerospace Materials: Aluminum-Lithium Alloys

K.T. Venkateswara Rao and R.O. Ritchie

October 1988

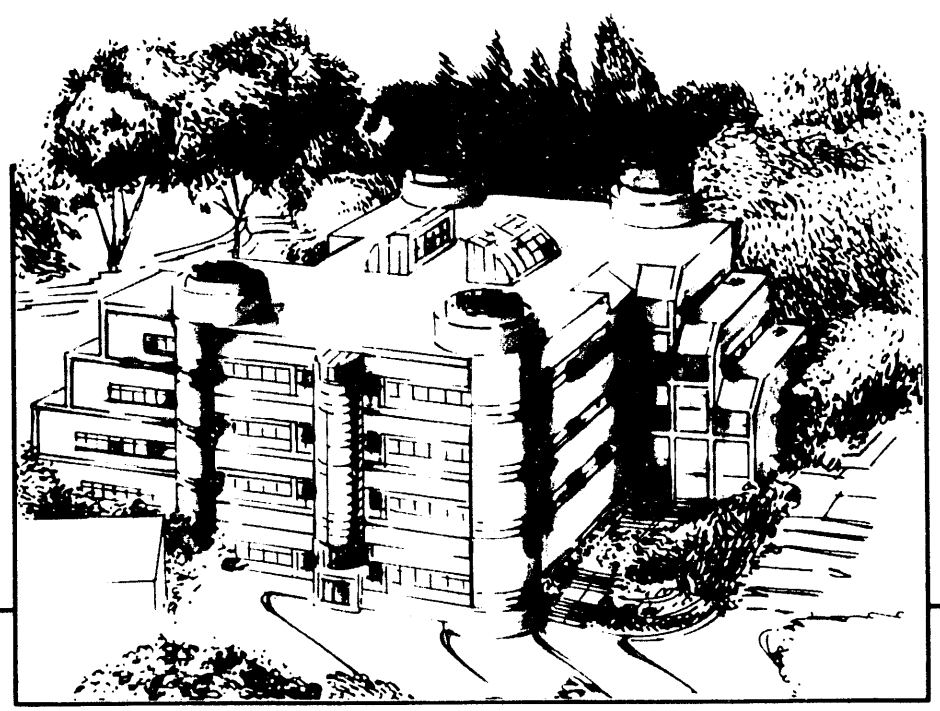

Materials and Chemical Sciences Division

Lawrence Berkeley Laboratory • University of California

ONE CYCLOTRON ROAD, BERKELEY, CA 94720 • (415) 486-4755

Prepared for the U.S. Department of Energy under Contract DE-AC03-76SF00098

DISCLAIMER

LBL--26298

DE92 000958

FATIGUE-CRACK PROPAGATION IN ADVANCED AEROSPACE MATERIALS: ALUMINUM-LITHIUM ALLOYS

K. T. Venkateswara Rao and R. O. Ritchie

Center for Advanced Materials, Lawrence Berkeley Laboratory
and
Department of Materials Science and Mineral Engineering
University of California, Berkeley, CA 94720, USA.

October 1988

presented at the Session on *Fracture and Fatigue of Advanced Aerospace Materials*, at the Seventh International Conference of Fracture (ICF-7), Houston, Texas, March 1989

Work supported by the Director, Office of Energy Research, Office of Basic Energy Sciences, Materials Sciences Division of the U.S. Department of Energy under Contract No. DE-AC03-76SF00098.

FATIGUE-CRACK PROPAGATION IN ADVANCED AEROSPACE MATERIALS: ALUMINUM-LITHIUM ALLOYS

K. T. VENKATESWARA RAO and R. O. RITCHIE

Center for Advanced Materials, Lawrence Berkeley Laboratory
and
Department of Materials Science and Mineral Engineering
University of California, Berkeley, CA 94720, USA.

ABSTRACT

Characteristics of fatigue-crack propagation behavior are reviewed for recently developed commercial aluminum-lithium alloys, with emphasis on the underlying micromechanisms associated with crack advance and their implications to damage-tolerant design. Specifically, crack-growth kinetics in Alcoa 2090-T8E41, Alcan 8090 and 8091, and Pechiney 2091 alloys, and in certain powder-metallurgy alloys, are examined as a function of microstructure, plate orientation, temperature, crack size, load ratio and loading sequence. In general, it is found that growth rates for long (> 10 mm) cracks are nearly 2-3 orders of magnitude slower than in traditional 2000 and 7000 series alloys at comparable stress-intensity levels. In addition, Al-Li alloys show enhanced crack-growth retardations following the application of tensile overloads and retain superior fatigue properties even after prolonged exposure at overaging temperatures; however, they are less impressive in the presence of compression overloads and further show accelerated crack-growth behavior for microstructurally-small (2-1000 μm) cracks (some three orders of magnitude faster than long cracks). These contrasting observations are attributed to a very prominent role of crack-tip shielding during fatigue-crack growth in Al-Li alloys, promoted largely by the tortuous and zig-zag nature of the crack-path morphologies. Such crack paths result in *locally* reduced crack-tip stress intensities, due to crack deflection and consequent crack wedging from fracture-surface asperities (roughness-induced crack closure); however, such mechanisms are far less potent in the presence of compressive loads, which act to crush the asperities, and for small cracks, where the limited crack wake severely restricts the shielding effect.

KEYWORDS

Aluminum-lithium alloys, fatigue-crack propagation, variable-amplitude loading, small cracks, microstructure effects, crack-tip shielding (crack deflection, crack closure)

INTRODUCTION

Due primarily to potential weight and fuel savings, low-density, high-strength, lithium-containing aluminum alloys are currently of great interest to the aerospace industry (Sanders and Starke, 1981, 1984; Baker *et al.*, 1986; Champier *et al.*, 1987). Despite early problems with poor ductility and fracture properties, recent advances in alloy design and

thermomechanical processing have led to optimized chemistries and microstructures, with the result that modern commercial aluminum-lithium alloys exhibit attractive strength-toughness combinations (Starke *et al.*, 1981; Harris *et al.*, 1984; Gregson and Flower, 1985; Jata and Starke, 1986), particularly at cryogenic temperatures (Webster, 1984; Glazer *et al.*, 1986; Dorward, 1986; Venkateswara Rao *et al.*, 1988c).

Of the I/M alloys studied, quaternary Al-Li-Cu-Zr and quinternary Al-Li-Cu-Mg-Zr systems have shown the most promise; alloys of commercial interest from these systems are registered as 2090, 8090, 8091 and 2091, with the compositions listed in Table I. 2090 and 8091 are considered as high-strength substitutes for Al-Zn-Cu-Mg (7XXX) alloys, whereas 2091 and 8090 are projected for medium strength and damage-tolerant applications replacing Al-Cu-Mg (2XXX) alloys. Presently, these alloys are undergoing comprehensive testing and evaluation for various aerospace and cryogenic tankage applications; in fact, certain Al-Li components are already in use in existing aircraft structures (Wakeling *et al.*, 1988).

Results to date suggest that the fatigue-crack growth properties of Al-Li alloys are generally superior to traditional 2000 and 7000 series alloys, an observation which has been rationalized in terms of their higher elastic modulus, which reduces crack-tip opening displacements (CTODs) (Harris *et al.*, 1984), and their ease of slip reversibility from the shearable nature of coherent δ' (Al_3Li) precipitates (Coyne *et al.*, 1981; Jata and Starke, 1986). However, the marked planarity of slip also promotes deflected and tortuous crack-path morphologies, resulting in enhanced wedging of the crack by fracture-surface asperities (roughness-induced crack closure). Such crack deflection and associated crack-closure mechanisms (Fig. 1) are considered to be more significant in contributing to the superior fatigue resistance in Al-Li alloys as they act to inhibit crack-growth kinetics by *locally* reducing the stress intensities experienced at the crack tip, i.e., by crack-tip shielding (Ritchie, 1988).

The superior fatigue-crack growth resistance of Al-Li alloys, however, has been based largely on standard tests involving fracture-mechanics type specimens containing long (> 10 mm) through-thickness cracks, generally tested at constant-amplitude loads at low positive load ratios. Although such studies provide important baseline data which permit an understanding of the role of microstructure and of the prevailing crack-advance mechanisms, they do not necessarily reflect service conditions, nor do they present a complete assessment of fatigue resistance. For example, the service lifetime of many fatigue-critical components consists of variable-amplitude loads or, alternatively, is controlled by the growth of cracks which are microstructurally or physically small (typically < 1 mm). In assessing fatigue performance, it is thus vital to examine the role of such factors as crack size, load ratio and loading sequence. This is particularly significant for aluminum-lithium alloys as they derive

their superior crack-growth properties extrinsically by crack-tip shielding and such shielding is known to be critically dependent upon crack size, geometry, CTOD, and loading sequence.

The intent of this paper is therefore to review the fatigue-crack growth properties of commercial aluminum-lithium alloys, with respect to variations in microstructure, crack size, temperature, load ratio and loading sequence, and to compare results with that of traditional 2124-T351 and 7150-T651 alloys. It is found that unlike 2124 and 7150, Al-Li alloys exhibit an extremely prominent role of crack-tip shielding, which largely accounts for their unique crack-propagation behavior.

MATERIALS AND MICROSTRUCTURES

Commercial 11-16 mm thick plates of aluminum-lithium alloys 8090 and 8091 (cast by Alcan) and 2091 (Pechiney) were tested in their recommended peak aged (T8X) and naturally aged (T351) tempers, whereas 2090 (Alcoa) was tested in an experimental T8E41 (near-peak aged) condition; results were compared with traditional high-strength aluminum alloys 2124-T351 and 7150-T651. Chemical compositions and corresponding heat treatments are listed, respectively, in Tables I and II.

Grain structures in most high-strength aluminum alloys are pan-cake shaped and elongated in the rolling direction; Al-Li alloy plate, however, shows a greater degree of anisotropy, generally without recrystallization due to small Zr additions. This is shown by the three-dimensional optical micrographs of 2090, 8090, 8091 and 2091 in Fig. 2. Grain sizes are fairly coarse, typically 500 μm wide by 50 μm thick by several mm long, except in 8091, where they were considerably finer; all alloys are unrecrystallized except for a small degree in 2091. Strong deformation textures are common in these alloys owing to prior thermomechanical treatments (the alloys are generally stretched 3 to 6% before aging to suppress grain-boundary precipitation); these textures have been found to be predominantly of the "brass" type ($\{110\}<112>$), with evidence of weaker "S" ($\{123\}<634>$) and "copper" ($\{112\}<111>$) types (Hirsch *et al.*, 1987; Vasudévan *et al.*, 1988; Yoder *et al.*, 1988).

Underaged Al-Li alloys are strengthened by fine, homogeneous, matrix distributions of coherent, ordered, spherical $\delta'(Al_3Li)$ precipitates and ß' (Al_3Zr) dispersoids. In 2090, aging to peak strength leads to coarsening of δ' precipitates and to matrix precipitation of T_1 (Al_2CuLi) and Θ'-like (Al_2Cu) plates (Fig. 3a); also evident is fine precipitation of T_1 plates along sub-grain boundaries (Fig. 3b), with less than ~100 nm wide δ'-precipitate free zones (PFZs). In Mg-containing alloys (except 2091), T_1 and Θ' plates are replaced by S (Al_2CuMg) or S' (precursor to S) laths in the matrix (Fig. 3c). In 8090-T8X, this causes some precipitation along high-angle grain boundaries and consequent formation of small (~500 nm) δ'-PFZs (Fig. 3d);

in 8090-T8X, grain-boundary precipitation is more extensive and PFZs are correspondingly wider (~ 1 μm). In 2091, artificial aging merely coarsens matrix δ'-precipitates; no other evidence of precipitation is apparent. Microstructural details and room-temperature mechanical properties are summarized in Tables III and IV, respectively.

FATIGUE-CRACK PROPAGATION BEHAVIOR

Long-Crack Behavior

Crack-Growth-Rates. Constant-amplitude long-crack fatigue behavior is generally determined with fracture-mechanics type geometries, e.g., compact C(T) specimens, containing long (> 10 mm) through-thickness cracks. Typical growth-rate results, as a function of the nominal stress-intensity range ($\Delta K = K_{max} - K_{min}$), are shown in Fig. 4a for peak aged 2090, 8090, 8091 and 2091 alloys (L-T orientation at a load ratio $R = K_{min}/K_{max}$ of 0.1); data are compared with 2124-T351 and 7150-T651. Corresponding crack-closure levels, measured using back-face strain compliance methods (Ritchie and Yu, 1987) as the closure stress intensity, K_{cl}, at first contact of the fracture surfaces on unloading, normalized with respect to K_{max}, are shown in Fig. 4b.

The Al-Li alloys can be seen to display consistently slower crack velocities over the entire spectrum of growth rates, except perhaps at near-threshold levels compared to 2124-T351. Such behavior is attributed primarily to their higher crack-closure levels (Fig. 4b) which, unlike traditional alloys, remain significant even at higher growth rates; in 2090-T8E41 for instance K_{cl}/K_{max} ratios remain over 0.5 for ΔK levels as high as 7-8 MPa$\sqrt{m}$.

The high closure levels can be attributed primarily to the meandering and tortuous nature of cyclic crack-path morphologies in these alloys (Venkateswara Rao *et al.*, 1988a), as illustrated in Fig. 5. Qualitatively, fracture surfaces in 2090, 8090 and 2091 are unduly rough and covered with transgranular shear facets, representative of highly deflected crack paths. In 8091, however, which exhibits the lowest closure levels and fastest growth rates, crack paths are essentially linear; 2090-T8E41, conversely, develops the highest closure levels and correspondingly shows the highest resistance to fatigue-crack growth.

In addition to crack-tip shielding, the superior fatigue-crack growth properties of aluminum-lithium alloys have been attributed to the $\sim 15\%$ higher modulus (compared to traditional Al alloys), which reduces the crack-tip opening displacements per cycle (Harris *et al.*, 1984), and to an increased reversibility of crack-tip deformation due to the marked planarity of slip, which reduces the degree of fatigue "damage" per cycle (Coyne *et al.*, 1981). Such processes undoubtedly act in concert with the effect of crack path described above,

although latter mechanism, based on crack-tip shielding, appears to be the most convincing, in view of the high measured levels of crack closure and observed effects of crack size, load ratio and loading sequence (Vasudévan and Suresh, 1985; Petit *et al.*, 1986; Venkateswara Rao *et al.*, 1988a,b; Venkateswara Rao and Ritchie, 1988a,b). In essence, the meandering crack paths in Al-Li alloys (see below) lead to slower (long-crack) growth rates a) by increasing the path length of the crack, b) by reducing the local K levels from crack deflection by deviation of the crack from the principal stress plane (Suresh, 1983), and c) by reducing the local ΔK level by enhancing (roughness-induced) crack closure due to the wedging of the crack by enlarged fracture-surface asperities (Fig. 6) (Venkateswara Rao and Ritchie, 1988b).

Investigations of a more fundamental nature on single crystals and polycrystalline samples of binary aluminum-lithium alloys reveal that cyclic stresses result in shear of coherent δ'-particles (Brechet *et al.*, 1987; Gentzbittel *et al.*, 1987); cumulative damage is then the result of mutual competition between the resultant dissolution and fatigue-induced coalescence of these precipitates. Such reversions and reprecipitation of δ'-precipitates caused by dislocation shear are responsible for the stress instabilities seen on hysteresis loops of low-cycle fatigue specimens cycled under constant strain (referred to as fatigue-induced strain-age hardening phenomenon (Gentzbittel *et al.*, 1987)). Although the precise relevance of such microscopic processes to crack-advance mechanisms in commercial alloys is as yet unclear, these observations confirm that cyclic deformation proceeds by dislocation shearing of the δ' precipitates, and of S'-laths in 8090-type alloys (Khireddine *et al.*, 1988), which promotes the faceted crack-path morphology so characteristic of planar-slip materials.

Crack-Path Morphology. The shearable nature of the strengthening precipitates results in inhomogeneous (planar slip) deformation, where strain is localized along narrow persistent slip bands (PSBs). Although such localized planar-slip deformation can lead to reduced toughness, particularly when coupled with embrittled grain boundaries, and to reductions in low-cycle fatigue (crack initiation) resistance, it can improve crack-growth properties through enhanced crack-tip shielding promoted by the resulting crystallographically deflected and tortuous crack-path morphologies. As shown in Fig. 7a for the L-T orientation in alloy 2090-T8E41, this can lead to macroscopic crack branching, where the entire crack deflects at an angle to the principal stress plane; alternatively, crack growth can be faceted, where the crack path shows periodic "zig-zags" (Fig. 7b). The anisotropic, pan-cake shaped grain structures can induce a further form of deflection in the short-transverse (S-L, S-T) orientations (Fig. 7c), specifically by linkage between intergranular delamination cracks.

The pronounced deformation textures in Al-Li alloys can also promote crack deflection. Fig. 8 shows the profile of the faceted fatigue fracture surface across the specimen thickness,

taken perpendicular to the fracture surface and crack-growth direction. Texture analysis shows that the sharp crystallographic facets, with an included angle of ~60°, are a result of deformation or crack growth along two sets intersecting (111) slip bands (Yoder *et al.*, 1988).

It is the combined effects of branching and roughness-induced crack closure, due to crack deflection (planar-slip induced) and crack-path tortuosity (deformation-texture induced), which are primarily responsible for the high levels of crack-tip shielding in aluminum-lithium alloys (Venkateswara Rao *et al.*, 1988a). As these phenomena persist up to high ΔK levels, unlike traditional alloys, the resultant beneficial influence on crack-growth rates is not solely confined to the near-threshold regime.

Plate-Orientation Effects

One consequence of long-crack fatigue properties alloys being closely related to crack-path morphology is that fatigue-crack growth rates in Al-Li alloys are strongly anisotropic; microstructurally, this is primarily associated with deformation texture, shape of the grain structure, and the nature of the grain-boundary chemistry and PFZs. Accordingly, nearly four orders of magnitude difference in growth-rate behavior exists in plate 2090 alloy (at fixed ΔK levels) between the various orientations; such variations are consistent with correspondingly large differences in crack closure (Fig. 9).

In-plane L-T, T-L and L+45° (LT-TL) orientations, which develop the highest crack-closure levels (i.e., K_{cl} values approach ~90% K_{max}) from the most deflected transgranular crack paths, show the slowest growth rates, with threshold ΔK_{TH} values between 3-4 MPa$\sqrt{m}$; similarly, crack-growth resistance is high for the T-S orientation where crack advance can be deflected through ~90° as it follows the weak short-transverse grain boundaries. Conversely, in the S-L and S-T orientations, the crack faces a microstructure of predominantly grain-boundary surface weakened by the presence of Fe- and Cu-rich intermetallics and possibly Na and Li segregation (Vasudévan *et al.*, 1984; Miller *et al.*, 1986); in following these boundaries, the intergranular crack path is essentially linear, the lowest closure levels are developed, and growth rates are consequently the fastest. The lowest threshold (ΔK_{TH} = 2.4 MPa$\sqrt{m}$), however, is found for the L+45° orientation, which shows a somewhat reduced modulus and ~16% lower strength.

Microstructural Effects

Microstructural effects on fatigue-crack growth in Al-Li alloys are not dissimilar to other precipitation-strengthened Al alloys. Growth rates in underaged structures are generally

slower, due to a marked planarity of slip from the coherent (shearable) precipitate distribution, which promotes deflected crack paths and hence high crack-closure levels. On artificial aging, deformation becomes more homogeneous as the precipitates become less coherent; growth rates are now generally faster as the reversibility of slip, the crack-path tortuosity and resulting crack-closure levels are all diminished. However, the δ'-precipitates in Al-Li alloys remain coherent up to large particle diameters; optimum fatigue properties can thus be attained at peak tempers, provided grain-boundary precipitation and associated PFZ formation is largely suppressed (Venkateswara Rao and Ritchie, 1988b,c)

As noted above, growth rates in microstructures which develop high shielding levels are generally lower; this is clearly illustrated by the T8 tempers of 2090, 8090, 8091 and 2091 (Figs. 4,5). Factors which affect the *intrinsic* fatigue-crack growth resistance, conversely, appear to be quite limited, as shown by the closure-corrected data for the four alloys plotted in terms of ΔK_{eff} in Fig. 10; apart from behavior close to ΔK_{TH}, growth rates in both the T3 and T8 tempers of all alloys are fairly similar.

Load-Ratio Effects

It is well known that higher load ratios (at equivalent ΔK levels) lead to increased fatigue-crack propagation rates, particularly at near-threshold levels (e.g., Ritchie and Yu, 1987), and that the effect is primarily associated with a diminished role of crack closure from the larger crack opening displacements. This dependency on load ratio is particularly marked in Al-Li alloys as closure levels are high, but can be completely normalized by characterizing growth rates in terms of ΔK_{eff} rather than ΔK, after allowing for the crack-face contact (Fig. 11). However, owing to this limited influence of crack closure at high load ratios, the superior (long-crack) fatigue-crack growth properties of Al-Li alloys are far less apparent (Fig. 12); the superiority of Al-Li alloys is similarly muted for tension-compression cycling ($R = -1$) as the compressive loads can act to limit (roughness-induced) crack closure through the crushing of asperities (Yu and Ritchie, 1987).

Small-Crack Behavior

Studies of naturally-occurring, microstructurally-small (2-1000 μm) surface fatigue cracks in Al-Li alloys indicate that cracks initiate at structural heterogeneities, typically Fe-Cu rich inclusions, constituent phases or second-phase particles, and grow along surface slip bands (Fig. 13). Their growth-rate response, as a function of ΔK, is shown in Figs. 14-16 and compared with conventional long-crack data. (Note: the use of K is appropriate here as

computed maximum and cyclic plastic zone sizes remain small (typically 4%) compared to crack size). In Fig. 14 where results are shown for underaged and peak-aged 2091, it is apparent that small cracks propagate at rates as much as 2-3 orders of magnitude faster than long cracks at equivalent ΔK levels; moreover, small-crack growth is seen at ΔK levels as low as 0.8 MPa$\sqrt{m}$, far below the threshold ΔK_{TH} for no long-crack growth (Venkateswara Rao *et al.*, 1986, 1988b; James, 1987).

A principal reason for the large discrepancy between the growth-rate behavior of long and small flaws is the minimal crack-tip shielding associated with small cracks of limited wake. This can be appreciated by comparing small-crack results with long-crack data which have been corrected for closure, i.e., after replotting in terms of ΔK_{eff}, as shown for the 2090 alloy in Fig. 15. It can be seen that the small-crack growth rates more closely correspond to long-crack da/dN vs. ΔK_{eff} data, indicating that small-crack effects result primarily from their reduced closure levels. However, once a substantial crack wake is established, typically in Al-Li alloys at crack sizes above $\sim$700 μm, long- and small-crack data essentially merge as shielding levels become equivalent.

In contrast to long-crack behavior where microstructural effects clearly influence growth rates (Figs. 4,9,12), minimal effects of alloy chemistry and microstructure are apparent for small-crack behavior in Al-Li alloys, although the degree of scatter is far larger (Fig. 16). This implies that the salient role of microstructure in the fatigue of these alloys is largely through the development of crack-tip shielding, consistent with the fact that once shielding is suppressed, i.e., at high load ratios (Fig. 12) or when plotting in terms of ΔK_{eff} (Fig. 10), microstructural effects are diminished. However, since the long-crack behavior of Al-Li alloys is generally superior to all other high-strength aluminum alloys, primarily due to large contributions from shielding, differences in long- and small-crack results are perhaps most significant in these alloys. Aluminum-lithium alloys thus show the best long-crack properties and anomalously high small-crack growth rates, paradoxically for the same reason - crack-tip shielding.

Variable Amplitude Loading

The prominence of crack-tip shielding during fatigue-crack growth in Al-Li also confers superior resistance to tensile-dominated variable amplitude loading. Shown in Fig. 17 are the effects of 50, 100 and 150% single tensile overloads on crack-growth rates in 2090-T8E41 at a constant baseline stress-intensity range of 8 MPa$\sqrt{m}$. Although 50% overloads have little influence, the larger overloads result in a characteristic brief, yet immediate, acceleration

followed by crack arrest or, in the present instance, a period of prolonged retardation before growth rates return to their baseline value (Venkateswara Rao and Ritchie, 1988a).

Recent mechanistic studies in these alloys (Ward-Close and Ritchie, 1988; Venkateswara Rao and Ritchie, 1988a) have indicated that the delay is associated with residual compressive stresses in the overload plastic zone and the consequent enhanced crack closure *in the immediate vicinity of the crack tip* as the crack grows into the zone. The superior properties of Al-Li, compared to traditional 2124-T3 and 7050-T6 alloys (Fig. 18), may also be associated with extensive surface crack branching and deflection at the overload.

These results are consistent with the superior performance of Al-Li alloys, compared to traditional alloys, under tension-dominated spectrum loading (Chanani *et al.*, 1986). Under compression-dominated spectra, however, they are less impressive (Yu and Ritchie, 1987). This has been attributed to the large contribution to fatigue-crack growth resistance from the wedging of enlarged fracture-surface asperities; under compressive loading, many asperities are crushed with a consequent decrease in closure. Such behavior has been reported for several aluminum alloys by applying compression overloads to cracks arrested at the threshold where the decrease in closure at the overload leads to crack advance at ΔK_{TH} (Zaiken and Ritchie, 1985); results for 2090-T8E41, however, indicate that the compression loads required for such crack growth are smallest in Al-Li alloys (Yu and Ritchie, 1987).

Higher Temperature Properties

A concern with aluminum alloys has been that prolonged exposure to moderately elevated temperatures (150° to 250°C) in certain applications can lead to severe overaging with a consequent loss in strength, ductility and fatigue performance. Studies up to 1024 h at 163°C show that the near-peak aged 2090 alloy suffers such a degradation with δ-grain-boundary precipitation, δ'-PFZ formation and matrix-precipitate coarsening; the result is a reduction in shielding levels as crack paths become more linear, and a consequent increase in growth rates (Venkateswara Rao and Ritchie, 1988c). The increase in crack-growth rates, however, is confined to above $\sim 10^{-9}$ m/cycle, and induces fatigue properties no worst than 2124-T3, 7150-T6 and 7150-T7 (Fig. 19).

Creep properties, conversely, may be better or worse than traditional 2219 and 2124 alloys depending upon orientation; growth rates in the T-L and L-T orientations can differ by almost six orders of magnitude, owing to strong texture and the anisotropy of the grain structure (Sadananda and Jata, 1988).

Corrosion Fatigue

Somewhat surprisingly, few studies to date have addressed the role of environment in influencing fatigue-crack growth in Al-Li alloys (Peters *et al.*, 1987; Haddleton *et al.*, 1987; Piascik and Gangloff, 1988; Pao *et al.*, 1988). In general, crack-growth rates are seen to be faster, and ΔK_{TH} values lower, in moist air and 3.5% NaCl solution compared to vacuum, with reduced slip-reversibility from environmental degradation considered as a major contributory mechanism (Jata and Starke, 1986). Thresholds in aqueous NaCl environments, however, are reported to be enhanced at low load ratios due to crack-wedging from corrosion products (Peters *et al.*, 1987). In general, it has been concluded that Al-Li alloys retain their superior (long-crack) fatigue properties even under sea-water environments, provided shielding from such crack-wedging phenomena can occur (Peters *et al.*, 1987; Pao *et al.*, 1988). However, at higher low ratios where wedge-shielding effects are minimized, their improved performance may be compromised at intermediate to high ΔK levels due to localized corrosion along slip bands or hydrogen-embrittlement mechanisms (Haddleton *et al.*, 1987).

To separate the extrinsic shielding effects from the chemical and electrochemical factors influencing corrosion fatigue in Al-Li alloys, more recent studies have examined the role of environment using physically-short cracks and long cracks cycled under constant-K_{max}/increasing-K_{min} conditions to suppress crack closure (Piascik and Gangloff, 1988a,b). Results for 2090-T8E41 show that water-vapor environments are most aggressive, followed by moist air and gaseous helium, gaseous oxygen having the least effect. Lower fatigue-crack growth rates were also seen at lower test frequencies, with cathodic polarization and with additions of Li_2CO_3, observations which were interpreted in terms of oxide/hydroxide surface films and hydrogen-embrittlement mechanisms. In general, however, the Al-Li alloys exhibited improved *intrinsic* corrosion-fatigue resistance compared to traditional alloys such as 7075-T6.

Powder-Metallurgy Alloys

The results discussed so far pertain to alloys processed by ingot-metallurgy (I/M) techniques, where compositions are constrained by the solid-solubility limits of alloying elements in aluminum. The powder-metallurgy (P/M) route, conversely, is not limited by such constraints and offers the possibility of developing alloys with unique compositions through such techniques as rapid solidification and mechanical alloying. The resulting P/M alloys often show remarkably high strength levels, yet fatigue-crack propagation rates are generally 1-2 orders of magnitude faster than in I/M alloys (Kemper *et al.*, 1987; Venkateswara Rao and

Ritchie, 1988d), as illustrated for the mechanically-alloyed Novamet Al-1.5Li-4Mg alloy (MA-905XL) in Fig. 20.

The reasons for the poor crack-growth properties of the P/M alloys can again be traced to limited crack-tip shielding. In essence, the very fine-scale microstructures (grain sizes are typically below $\sim 5\ \mu m$) result in linear crack paths (Fig. 20), which simply do not develop high levels of shielding by crack deflection and crack closure via asperity wedging as is seen in coarser-grained I/M materials. In fact, measured K_{cl} values at near-threshold levels are a mere 30% of K_{max} in the Novamet alloy, compared to ~90% in the I/M 2090-T8E41 alloy. Consequently, since closure levels are low, growth-rate behavior, and ΔK_{TH} values, in P/M alloys are relatively insensitive to load-ratio and geometry effects (see also Minakawa *et al.*, 1986; Kemper *et al.*, 1987).

DISCUSSION

The development of commercial aluminum-lithium alloys over the past five years has led to a series of monolithic aerospace materials with comparable properties and considerable price advantage over competing metal-matrix composite alloys. For example, plotted in Fig. 21 is a comparison of the fatigue-crack growth properties of 2090-T8E41 with a SiC-particulate reinforced P/M aluminum alloy and a aramid-fiber/epoxy resin/aluminum matrix laminate (ARALL-2). It is apparent that the laminate shows the best fatigue-crack growth properties; however, these properties are distinctly unidirectional, and the material is over three times more expensive than 2090. Similarly, Al-Li compares very favorably to the Al/SiC_p composite; the 2090 alloy exhibits superior crack-growth properties (except close to K_{TH}), and is again a less expensive material.

Extensive studies over the past few years make it clear that these excellent fatigue-crack propagation properties in Al-Li alloys are derived principally from an enhanced role of crack-tip shielding, rather than from any *intrinsic* role of microstructure. In the present work, it has been shown that such *extrinsic toughening*, whereby crack extension is impeded, not by increasing the microstructural crack-growth resistance, but rather by microstructural, mechanical and environmental mechanisms which act to reduce the *local* "crack driving force", is primarily the result of meandering, deflected and sometimes delaminated crack-path morphologies, which promote shielding both by crack deflection and resultant crack closure from the wedging of enlarged fracture-surface asperities. The origin of such tortuous crack paths in Al-Li alloys are coherent-particle hardened (planar slip) microstructures, which induce "zig-zag" slip-band cracking, the strong deformation texture, which can induce extensive crack

branching, and the weak short-transverse properties, which can cause delamination and crack splitting.

One important consequence of fatigue behavior dominated by crack-tip shielding is that such extrinsic toughening is not a material property. Thus, although significant crack deflection and closure induces long-crack growth properties, under both constant and tensile-dominated variable amplitude loading, which are superior to most other high-strength aluminum alloys, when such shielding mechanisms are inhibited, the superiority of Al-Li alloys can be lost. This can occur in several important situations: namely, at high load ratios, where the larger CTODs limit crack wedging; with small surface cracks or short cracks emanating from notches, where the restricted crack wake limits shielding in general; with compression overload cycles, where the compressive stresses act to crush fracture-surface asperities and limit closure; with excessive overaging, which promotes grain-boundary precipitation/PFZs and less deflected crack paths, and with P/M alloys, where the ultrafine grain sizes also inhibit crack deflection and subsequent closure. In addition, thin Al-Li alloy sheet (< 2 mm thick) appears to show significantly faster crack-growth rates than in nominally similar plate material (Bucci *et al.*, 1988), due primarily to a reduced propensity in thin sheet for crack deflection and splitting (texture is often reduced in sheet material because of recrystallization). Even testing center-cracked tension, rather than compact, DCB or bend, specimens may limit the superior fatigue performance of Al-Li alloys, as the former test geometry tends not to stabilize off-angle cracking and therefore inhibits highly deflected crack paths. A similar suppression of shielding in Al-Li alloys, with a consequent increase in crack-growth rates, has been seen by testing single-edged-notched tension specimens with fixed rather than freely rotating grips (Piascik and Gangloff, 1988a).

Finally, it should be noted that two of the main sources of crack-path tortuosity in Al-Li plate which confer the excellent fatigue-crack growth properties, namely the strong texture and weak short-transverse properties, may be considered undesirable for many applications. Attempts to develop new alloys with less anisotropy can clearly solve this problem, yet will undoubtedly result in fatigue-crack growth properties inferior to those exhibited by the present commercial alloys.

SUMMARY

The present paper has attemped to provide a characterization of the fatigue-crack propagation properties of commercial aluminum-lithium alloys, with specific emphasis on the micromechanisms which affect growth. It is reasoned that the excellent crack-growth resistance exhibited by these alloys in conventional "long-crack" tests can be attributed to very significant

contributions to crack-tip shielding, principally from crack deflection and resultant crack closure from the wedging of asperities, induced by the tortuous and deflected nature of the crack path. However, although these fatigue properties are better than any other monolithic high-strength aluminum alloy, it is further shown that where such shielding is inhibited, such as in certain orientations, at high load ratios, with small cracks, in the presence of compression overloads, with excessive overaging, and in thin sheet material, the superiority of Al-Li alloys may be compromised.

ACKNOWLEDGEMENTS

This work was supported through the Structural Materials Program in the Center for Advanced Materials by the Director, Office of Energy Research, Office of Basic Energy Sciences, Materials Sciences Division of the U.S. Department of Energy under Contract No. DE-AC03-76SF00098. The authors would like to thank numerous individuals who have contributed to this work, in particular Drs. R. J. Bucci, P. E. Bretz and R. R. Sawtell of Alcoa, P. Wakeling of Alcan, Drs. G. R. Chanani and G. V. Scarich of Northrop, Dr. W. E. Quist of Boeing, and Prof. P. P. Pizzo of San Jose State University, for providing materials and for helpful discussion. The assistance of Dr. W. Yu, H. Hayashigatani and J. E. Miles with the experiments, and Ms. Madeleine Penton with the preparation of the manuscript, is also gratefully acknowledged.

REFERENCES

Baker, C., P. J. Gregson, S. J. Harris and C. J. Peel, eds. (1986). *Aluminium-Lithium Alloys III*. Institute of Metals, London, U.K.

Brechet, Y., F. Louchet, C. Marchionni and J. L. Verger-Gaugry (1987). Experimental investigation and theoretical approach to the fatigue-induced dissolution of ' precipitates in a 2.5 wt % Al-Li alloy. *Phil. Mag. A*, 56, 353-366.

Bucci, R. J., P. L. Mehr, G. Sowinski, R. C. Malcolm, W. T. Kaiser and R. H. Wygonik (1988). Engineering and damage tolerance properties of 2090 Al-Li alloy sheet. In: *Aluminum-Lithium Alloys: Design, Development and Applications Update* (S. P. Agrawal *et al.*, eds.), ASM International, Metals Park, Ohio.

Champier, C., B. Dubost, D. Miannay and L. Sabetay, eds. (1987). *4th International Aluminium-Lithium Conference*. J. de Physique, Vol. 48:C3, No. 9. Les Editions de Physique, France.

Chanani, G. R., G. V. Scarich and K. M. Bresnahan (1986). Spectrum fatigue crack growth behavior of 2000 and 7000 series aluminum alloys. In: *Mechanical Properties and Phase Transformations in Engineering Materials* (S. D. Antolovich *et al.*, eds.), pp. 271-291. TMS-AIME, Warrendale, PA.

Coyne, E. J., T. H. Sanders and E. A. Starke (1981). The effect of microstructure and moisture on the low cycle fatigue and fatigue crack propagation of two Al-Li-X alloys. In: *Aluminum-Lithium Alloys* (T. H. Sanders and E. A. Starke, eds.), pp. 293-305. TMS-AIME, Warrendale, PA.

Dorward, R. C. (1986). Cryogenic toughness of Al-Cu-Li alloy AA 2090. *Scripta Metall.*, 20, 1379-1383.

Gentzbittel, J. M., G. Vigier and R. Fougeres (1987). The phenomenon of stress instabilities in Al-Li binary alloys and microscopic mechanisms connected. In: *4th International Aluminium-Lithium Conference* (G. Champier *et al.*, eds.), pp. 729-735. Les Éditions de Physique, France.

Glazer, J., S. L. Verzasconi, E. N. C. Dalder, W. Yu, R. A. Emigh, R. O. Ritchie and J. W. Morris (1986). Cryogenic mechanical properties of Al-Cu- Li-Zr alloy 2090. *Adv. Cryog. Eng.*, 32, 397-402.

Gregson, P. J. and H. M. Flower (1985). Microstructural control of toughness in aluminum-lithium alloys. *Acta Metall.*, 33, 527-537.

Haddleton, F. L., S. Murphy and T. J. Griffin (1988). Fatigue and corrosion fatigue of 8090 Al-Li-Cu-Mg alloy. In: *4th International Aluminium-Lithium Conference* (G. Champier *et al.*, eds.), pp. 809-815. Les Éditions de Physique, France.

Harris, S. J., B. Noble and K. Dinsdale (1984). Effect of composition and heat treatment on strength and fracture characteristics of Al-Li-Mg alloys. In: *Aluminum-Lithium Alloys II* (T. H. Sanders and E. A. Starke, eds.), pp. 219-233. TMS-AIME, Warrendale, PA.

Hirsch, J., O. Engler, K. Lücke, M. Peters and K. Welpmann (1987). The rolling texture development in an 8090 Al-Li alloy. In: *4th International Aluminium-Lithium Conference* (G. Champier *et al.*, eds.), pp. 605-611. Les Éditions de Physique, France.

James, M. R. (1987). Growth behavior of small fatigue cracks in Al-Li-Cu alloys. *Scripta Met.*, 21, 783-788.

Jata, K. V. and E. A. Starke (1986). Fatigue crack growth and fracture toughness behavior of an Al-Li-Cu alloy. *Metall. Trans. A*, 17A, 1011-1023.

Kemper, H., B. Weiss and R. Stickler (1987). Effect of compressive portion of loading cycles on the near threshold fatigue closure behavior. In: *Fatigue '87* (R. O. Ritchie and E. A. Starke, eds.), pp. 789-799. EMAS Ltd., Warley, U.K.

Khireddine, D., R. Rahouadj and M. Clavel (1988). Evidence of S' shearing in an aluminum-lithium alloy. *Scripta Metall.*, 22, 167-17[illegible].

Miller, W. S., M. P. Thomas, D. J. Lloyd and D. Creber (1986). Deformation and fracture in Al-Li base alloys. *Mater. Sci. Tech.*, 2, 1210-1216.

Minakawa, K., G. Levan and A. J. McEvily (1986). The influence of load ratio on fatigue crack growth in 7090-T6 and IN9021-T4 P/M aluminum alloys. *Metall. Trans. A*, 17A, 1787-1795.

Petit, J., S. Suresh, A. K. Vasudévan and R. C. Malcolm (1986). Constant amplitude and post-overload fatigue crack growth in Al-Li alloys. In: *Aluminium-Lithium Alloys III* (C. Baker *et al.*, eds.), pp. 257-262. Institute of Metals, London, U.K.

Pao, P. S., M. A. Imam, L. A. Cooley and G. R. Yoder (1988). Comparison of corrosion-fatigue cracking of Al-Li alloy 2090 and 7075-T651 in salt water. *Corrosion J.*, 102, in press.

Peters, M., V. Bachmann and K. Welpmann (1987). Fatigue crack propagation behavior of the Al-Li alloy 8090 compared to 2024. In: *4th International Aluminium-Lithium Conference* (G. Champier *et al.*, eds.), pp. 785-791. Les Éditions de Physique, France.

Piascik, R. S. and R. P. Gangloff (1988a). Intrinsic fatigue crack propagation in aluminum-lithium alloys: the effect of gaseous environments. In: *Proc. of 7th Intl. Conf. on Fracture* (K. Salama, ed.), Pergamon Press, NY, in press.

Piascik, R. S. and R. P. Gangloff (1988b). Aqueous environment effects on intrinsic corrosion fatigue crack propagation in an Al-Li-Cu alloy. In: *Proc. of Intl. Conf. on Environment-Induced Cracking of Metals*, in press.

Ritchie, R. O. (1988). Mechanisms of fatigue crack propagation in metals, ceramics and composites: role of crack tip shielding. *Mater. Sci. Eng.*, 103A, 15-28.

Ritchie, R. O. and W. Yu (1987). Short crack effects: a consequence of crack tip shielding. In: *Small Fatigue Cracks* (R. O. Ritchie and J. Lankford, eds.), pp. 167-189. TMS-AIME, Warrendale, PA.

Ritchie, R. O., W. Yu and J. Bucci (1988). Fatigue crack propagation in ARALL laminates: measurement of the effect of crack-tip shielding from crack bridging. *Eng. Fract. Mech.*, 25, in press.

Sadananda, K. and K. V. Jata (1988). Creep crack growth behavior of two Al- Li alloys. *Metall. Trans. A*, 19A, 847-854.

Sanders, T. H. and E. A. Starke, eds. (1981). *Aluminum-Lithium Alloys*. TMS- AIME, Warrendale, PA.

Sanders, T. H. and E. A. Starke, eds. (1984). *Aluminum-Lithium Alloys II*. TMS-AIME, Warrendale, PA.

Shang, J. K., W. Yu and R. O. Ritchie (1988). Role of silicon carbide particles in fatigue crack growth in SiC-particulate-reinforced aluminum alloy composites. *Mat. Sci. Eng.*, 102, 181-192.

Starke, E. A., T. H. Sanders and I. G. Palmer (1981). New approaches to alloy development in the Al-Li system. *J. Metals*, 32, 24-32.

Suresh, S. (1983). Crack deflection: implications for the growth of long and short fatigue cracks. *Metall. Trans. A*, 14A, 2375-2385.

Vasudévan, A. K. and S. Suresh (1985). Lithium-containing aluminum alloys: cyclic fracture. *Metall. Trans. A*, 16A, 475-477.

Vasudévan, A. K., A. C. Miller and M. M. Kersker (1984). Contribution of Na- segregation to fracture behavior of Al-11.4 at. % Li alloys. In: *Aluminum- Lithium Alloys II* (T. H. Sanders and E. A. Starke, eds.), pp. 181-199. TMS-AIME, Warrendale, PA.

Vasudévan, A. K., W. G. Fricke, R. C. Malcolm, R. J. Bucci, M. A. Przystupa and F. Barlat (1988). On through thickness crystallographic texture gradient in Al-Li-Cu-Zr alloy. *Metall. Trans. A*, 19A, 731-33.

Venkateswara Rao, K. T., W. Yu and R. O. Ritchie (1986). On the growth of small fatigue cracks in aluminum-lithium alloy 2090. *Scripta Metall.*, 20, 1459-1464.

Venkateswara Rao, K. T. and R. O. Ritchie (1988a). Mechanisms for the retardation of fatigue cracks following single tensile overloads: behavior in aluminum-lithium alloys. *Acta Metall.*, 36, 2849-2862

Venkateswara Rao, K. T. and R. O. Ritchie (1988b). Mechanical properties of commercial aluminum-lithium alloys: Part II. Fatigue crack propagation. *Mater. Sci. Technol.*, 4, in review.

Venkateswara Rao, K. T. and R. O. Ritchie (1988c). Effect of prolonged high- temperature exposure on the fatigue and fracture behavior of aluminum- lithium alloy 2090. *Mater. Sci. Eng.*, 100, 23-30.

Venkateswara Rao, K. T. and R. O. Ritchie (1988d). unpublished work.

Venkateswara Rao, K. T., W. Yu and R. O. Ritchie (1988a). Fatigue crack propagation in aluminum-lithium alloy 2090: Part I. Long crack behavior. *Metall. Trans. A*, 19A, 549-562.

Venkateswara Rao, K. T., W. Yu and R. O. Ritchie (1988b). Fatigue crack propagation in aluminum-lithium alloy 2090: Part II. Small crack behavior. *Metall. Trans. A*, 19A, 563-569.

Venkateswara Rao, K. T., H. F. Hayashigatani, W. Yu and R. O. Ritchie (1988c). On the fracture toughness of aluminum-lithium alloy 2090-T8E41 at ambient and cryogenic temperatures. *Scripta Metall.*, 22, 93-98.

Wakeling, P. O., S. D. Forness and E. A. W. Heckman (1988). The use of 8090 in the McDonnell-Douglas F15 SMTD aircraft. In: *Aluminum-Lithium Alloys: Design, Development and Application Update* (R. J. Kar *et al.*, eds.), pp. 339-340. ASM International, Metals Park, Ohio.

Ward-Close, C. M. and R. O. Ritchie (1988). On the role of crack closure mechanisms in influencing fatigue crack growth following tensile overloads in a titanium alloy: near threshold versus higher K behavior. In: *Mechanics of Fatigue Crack Closure, ASTM STP 982* (J. C. Newman and W. Elber, eds.), pp. 93-111. ASTM, Philadelphia, PA.

Webster, D. (1984). Aluminum-lithium alloys. *Metal Progress*, 125, 33-37.

Yoder, G. R., P. S. Pao, M. A. Imam and L. A. Cooley (1988). Prediction of slip-band facet angle in the fatigue crack growth of an Al-Li alloy. *Scripta Metall.*, 22, 1241-1244.

Yu, W. and R. O. Ritchie (1987). Fatigue crack propagation in 2090 aluminum- lithium alloy: effect of compression overload cycles. *J. Eng. Mater. Tech.*, 102, 81-85.

Zaiken, E. and R. O. Ritchie (1985). On the role of compression overloads in influencing crack closure and the threshold condition for fatigue crack growth in 7150 aluminum alloy. *Eng. Fract. Mech.*, 22, 35-48.

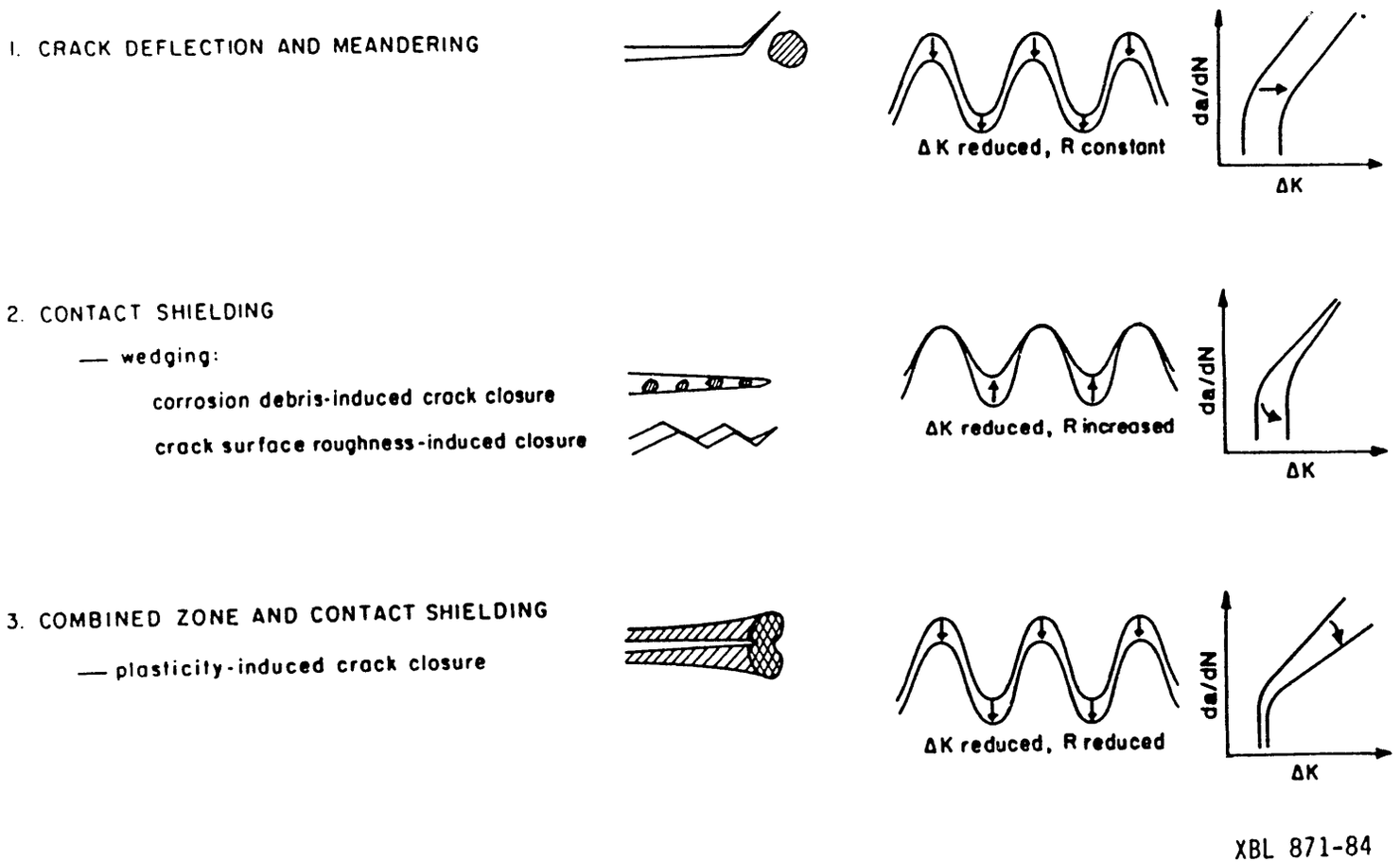

Fig. 1. Schematic illustration of the principal crack-tip shielding mechanisms influencing fatigue-crack propagation in aluminum-lithium alloys, and their consequences to crack-growth rate behavior (after Venkateswara Rao *et al.*, 1988a).

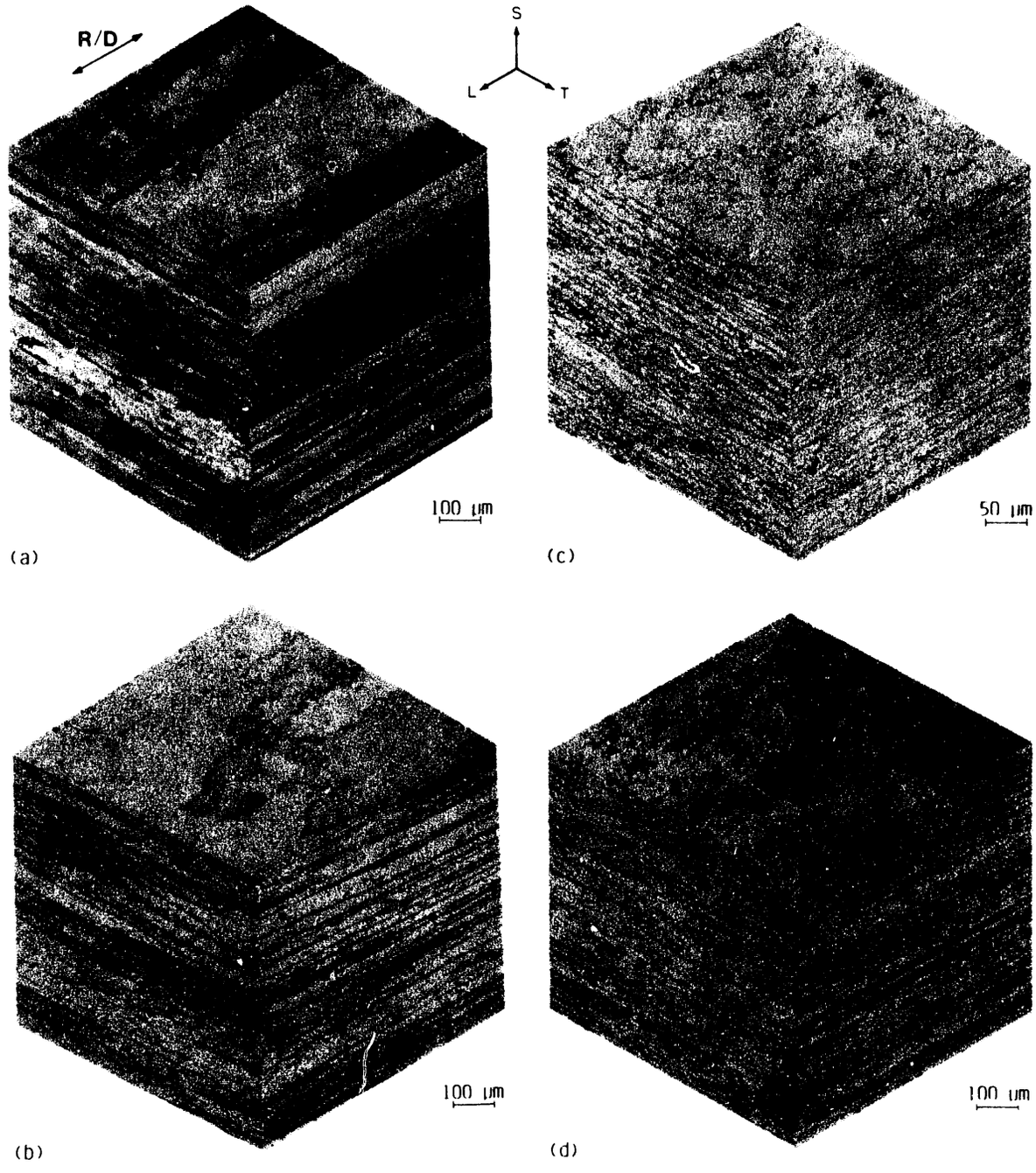

XBB 864-3075C

Fig. 2. Three-dimensional optical micrographs of commercial aluminum-lithium alloys a) 2090, b) 8091, c) 8090 and d) 2091, showing largely unrecrystallized and pan-cake shaped grain structures elongated along the rolling direction (Keller's reagent etch).

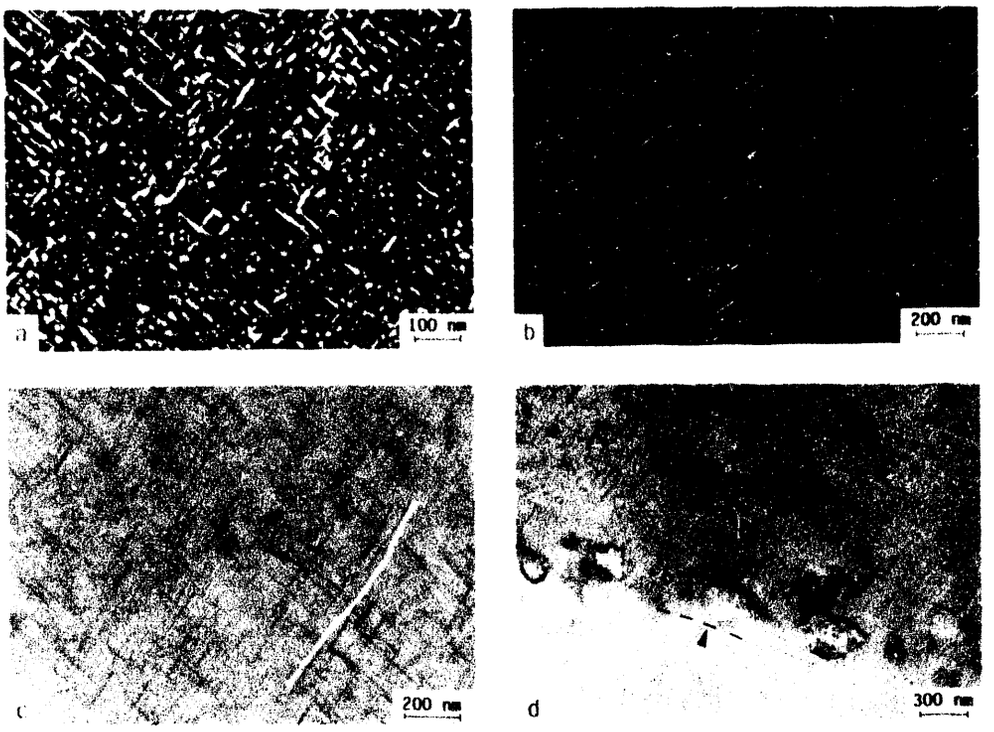

XBB 888-8249

Fig. 3. Transmission electron micrographs of the prominent microstructural features in commercial aluminum-lithium alloys. Centered dark-field images of a) δ', composite β'-δ' and Θ' precipitates, and b) T_1 plates in the matrix and along subgrain boundaries (indicated by arrows), in alloy 2090-T8E41; bright- field images of c) S' laths and d) δ'-PFZs (indicated by arrows) in alloy 8091-T8X. (Centered dark-field images in a,b) were obtained using the δ' and T_1 superlattice reflections, respectively.)

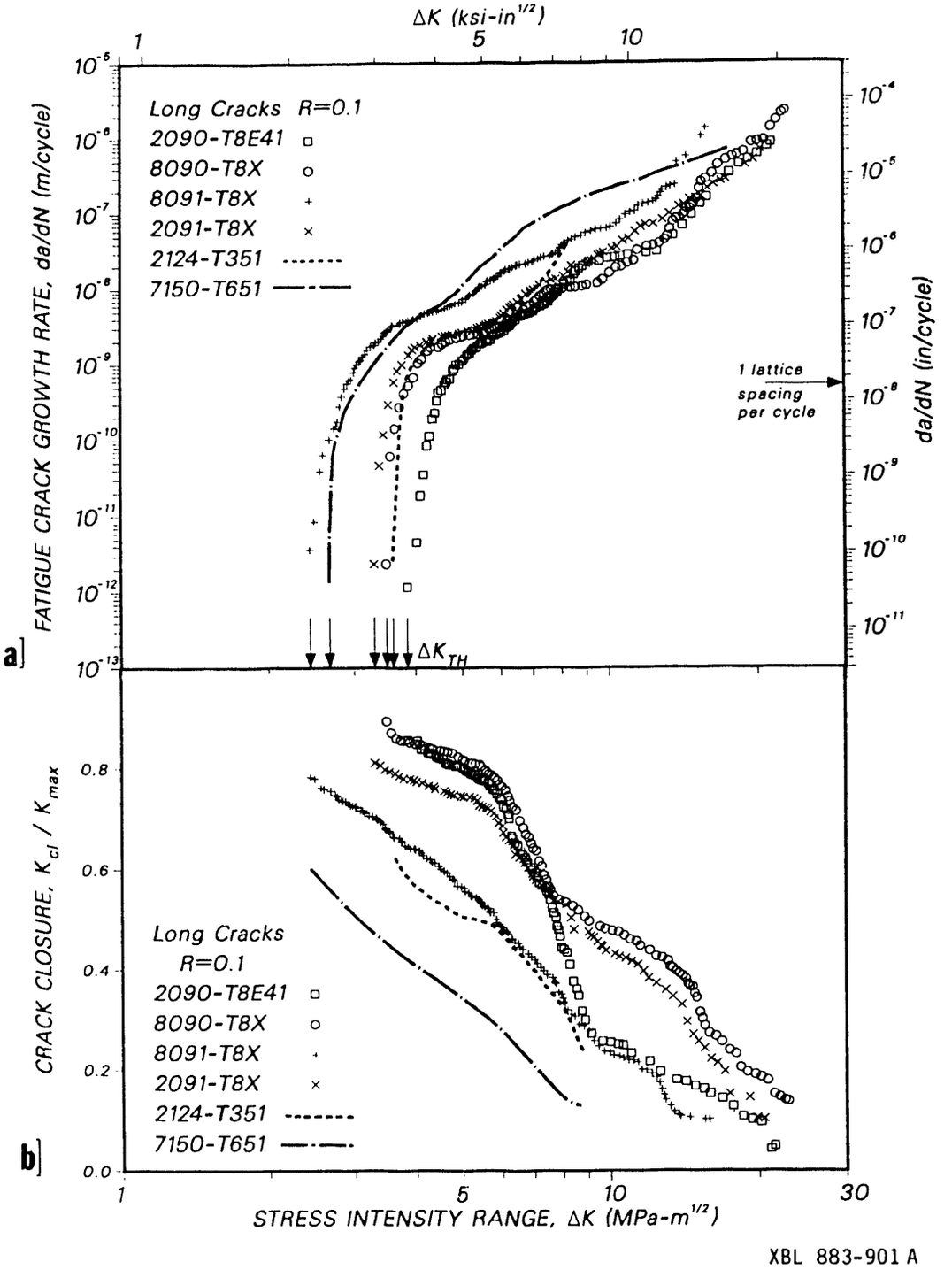

Fig. 4. Comparison of a) fatigue-crack growth rates and b) crack-closure levels for long cracks in commercial aluminum-lithium and conventional high-strength aluminum alloys (at R = 0.1). Note the general superiority of lithium-containing alloys, consistent with high crack-closure levels.

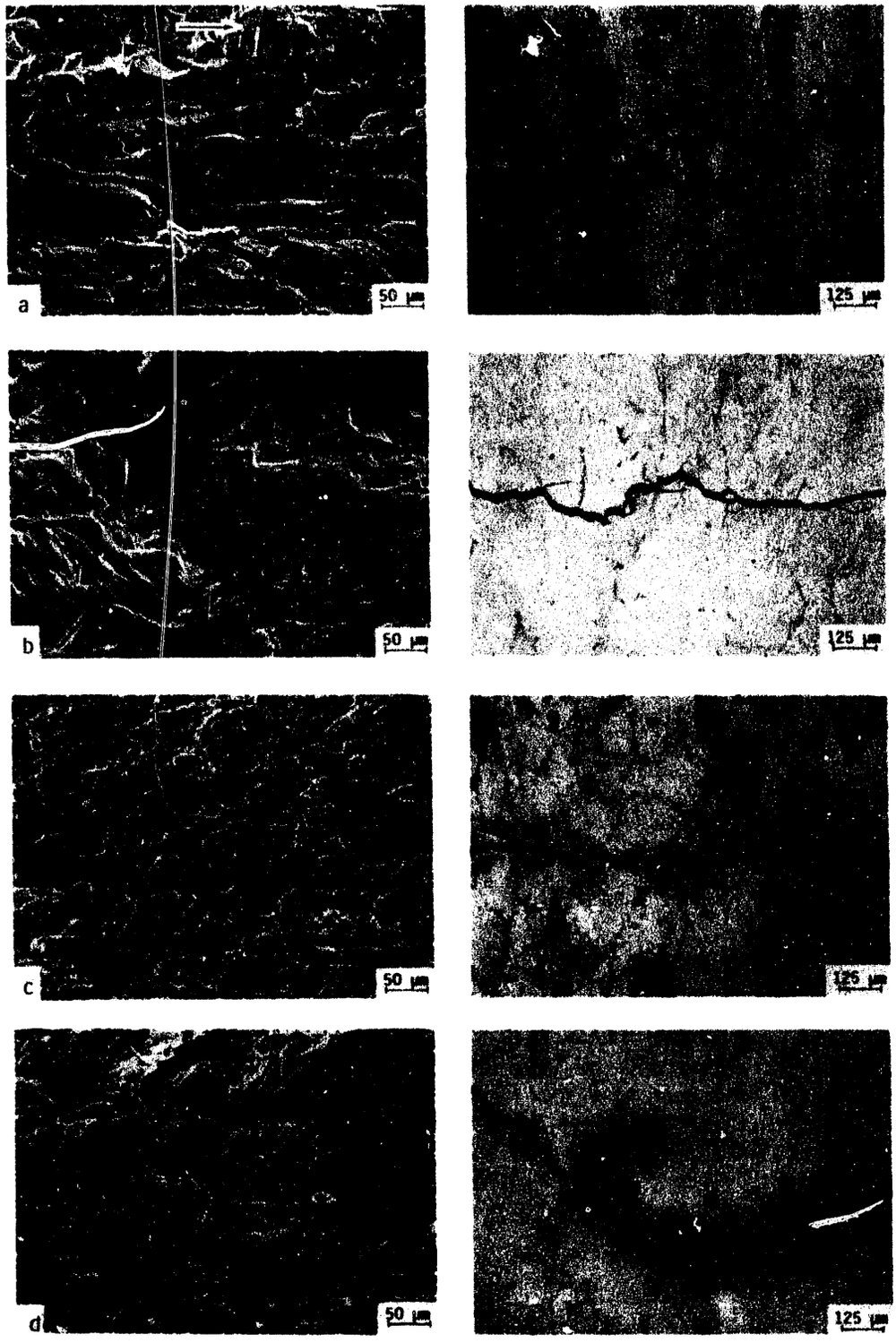

XBB 883-2387

Fig. 5. Scanning electron and optical micrographs of the fatigue fracture surfaces and crack-path morphologies, respectively, in a) 2090-T8E41, b) 8090-T8X, c) 8091-T8X and d) 2091-T8X alloys. Note the rough surfaces and deflected crack paths in 1090, 2091 and 8090, compared to the relatively flat fracture surface and linear crack path in 8091. Horizontal arrow indicates general direction of crack growth.

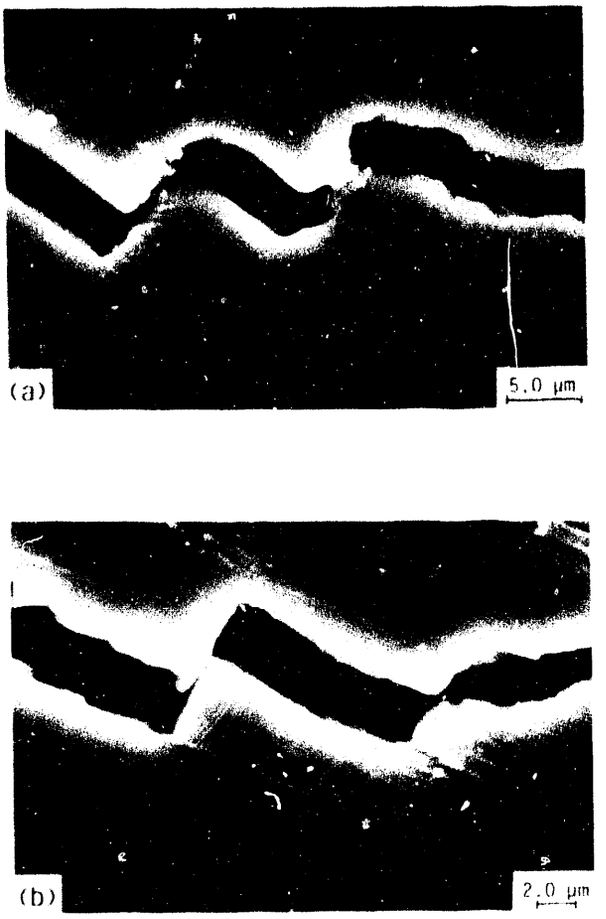

XBB 878-6961

Fig. 6. Meandering fatigue crack paths and resultant wedging of fracture-surface asperities (roughness-induced crack closure) in 2090-T8E41 aluminum-lithium alloy. Micrograph obtained from specimen surface; horizontal arrow indicates general direction of crack growth.

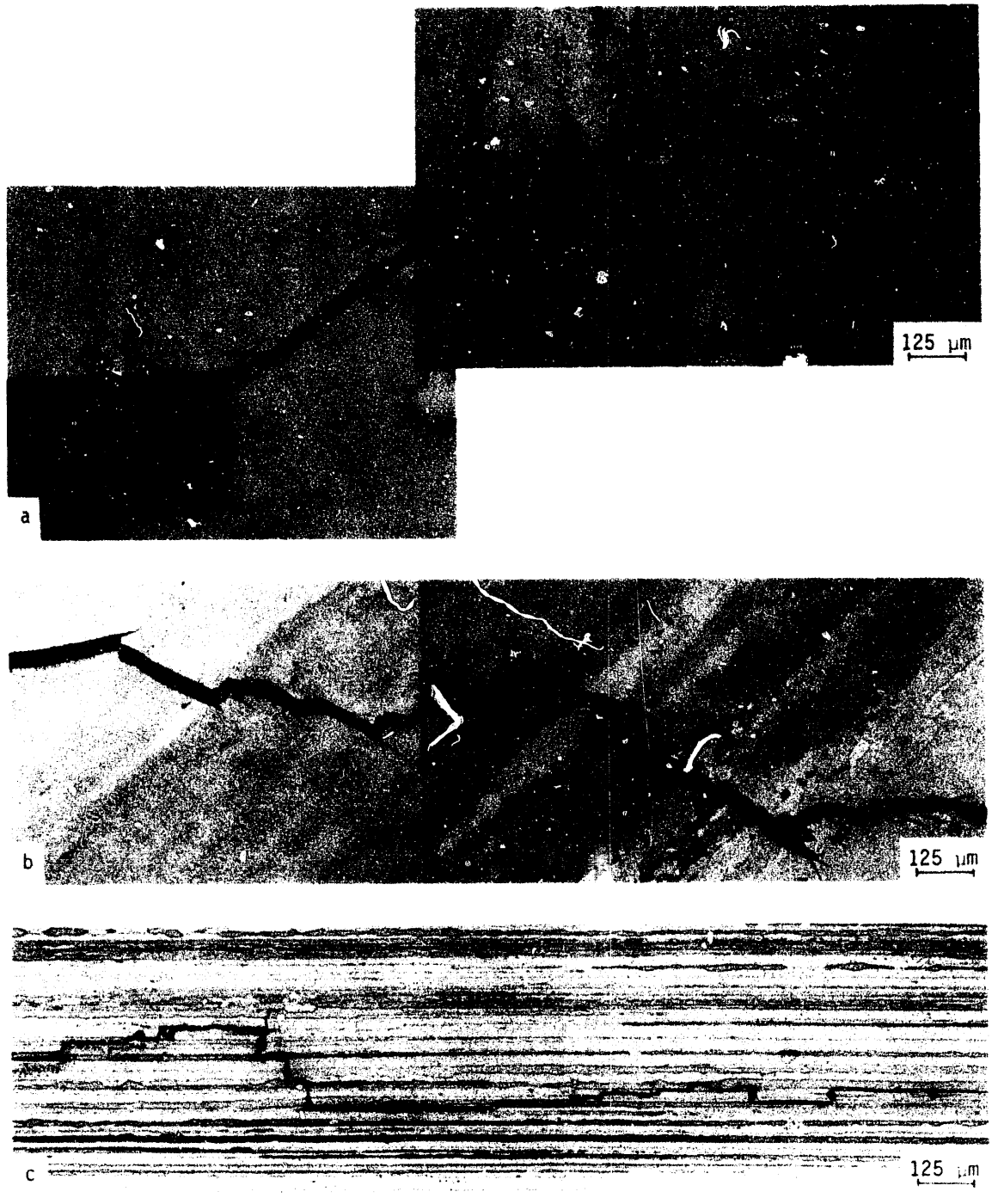

Fig. 7. Types of crack-path meandering during fatigue-crack propagation in Al-Li alloys, showing a) macroscopic crack branching, b) microscopic crack deflection (crystallographic slip-band cracking) and c) intergranular delamination (short-transverse) cracking in 2090-T8E41. Horizontal arrow indicates general direction of crack growth.

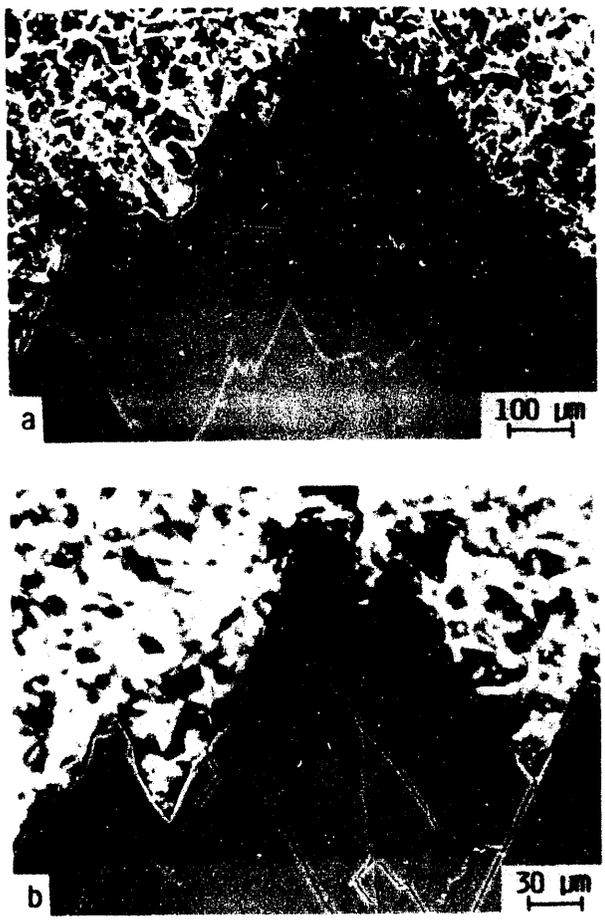

XBB 8811-11056

Fig. 8. Crystallographic crack-path tortuosity observed during fatigue-crack growth in Al- Li alloys induced by pronounced deformation texture. The sharp facets, with an included angle of ~60°, are a result of shearing along intersecting (111) planes through the thickness of the specimen. Micrograph obtained for 2090-T8E41 alloy in the L-T orientation by metallographically polishing sections taken normal to the crack-growth direction and the crack-growth plane.

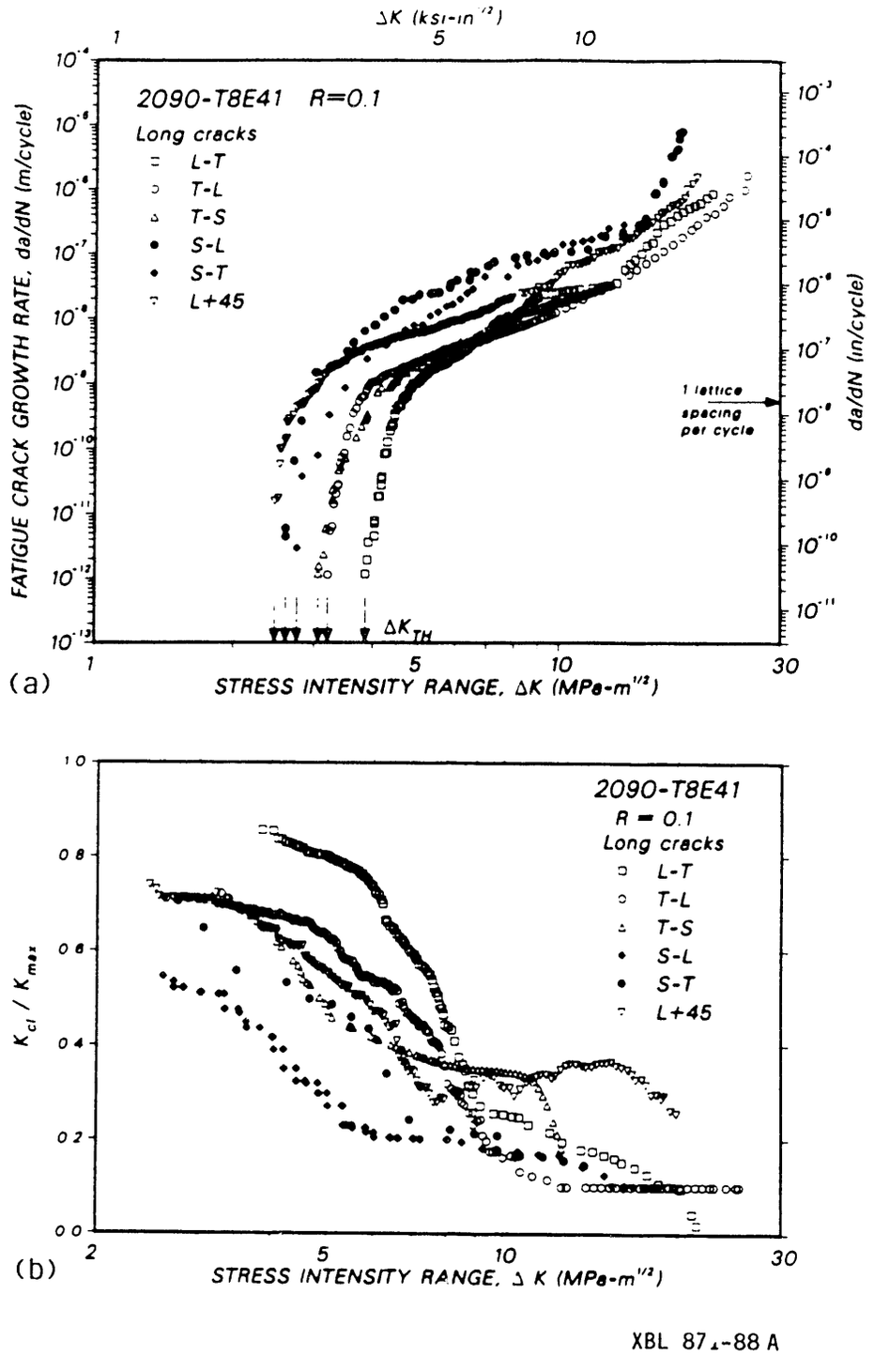

Fig. 9. Variation in a) fatigue-crack growth rates and b) crack-closure levels for long cracks in 2090-T8E41 alloy at R = 0.1, as a function of specimen oirientation. Note how growth rates parallel to the rolling plane (S-L, S-T) are the fastest, whereas growth rates normal to the rolling plane (L-T, T-S) are the slowest, consistent with the degree of crack-path tortuosity and resulting levels of crack closure.

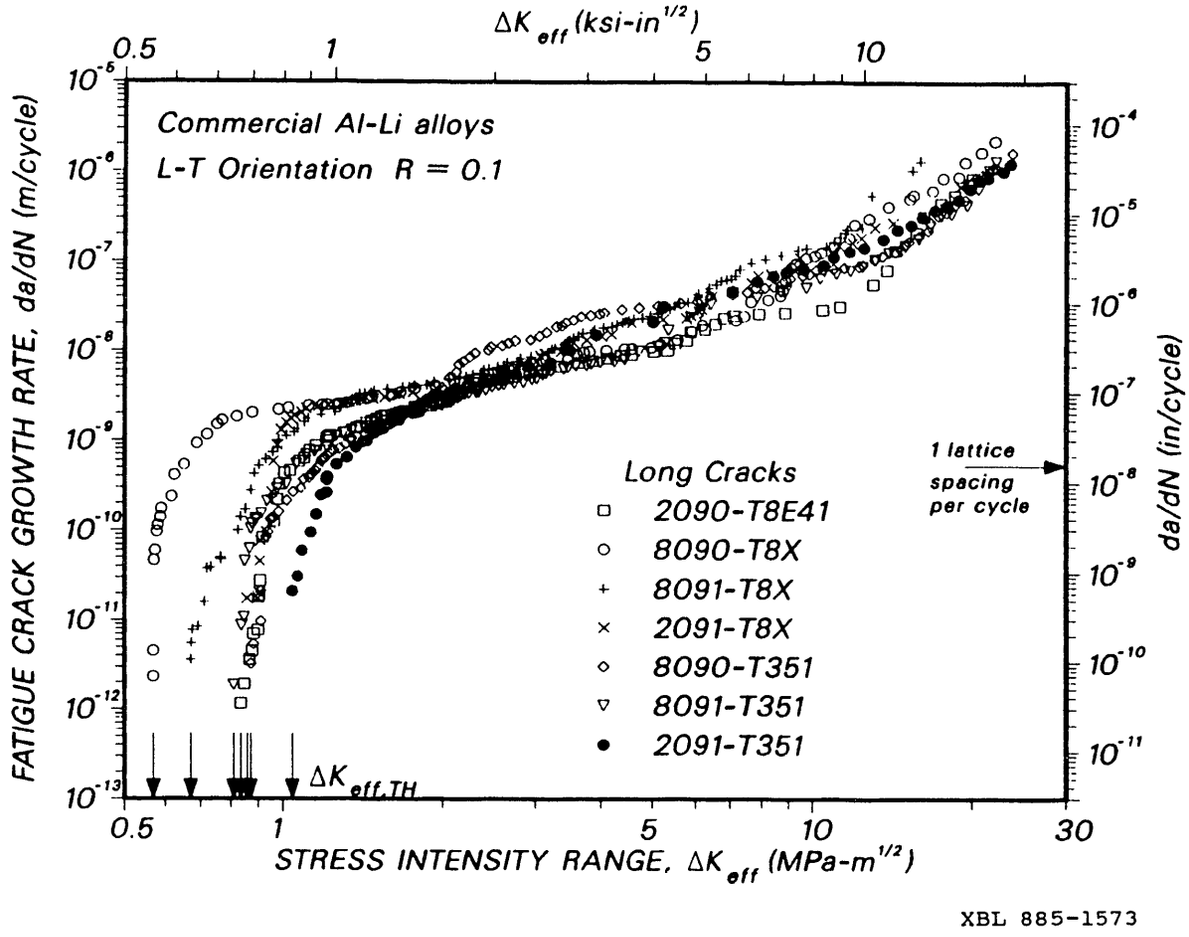

Fig. 10. Variation in fatigue-crack growth rates in commercial I/M aluminum-lithium alloys as a function of the effective stress-intensity range, ΔK_{eff}, after correcting for crack closure.

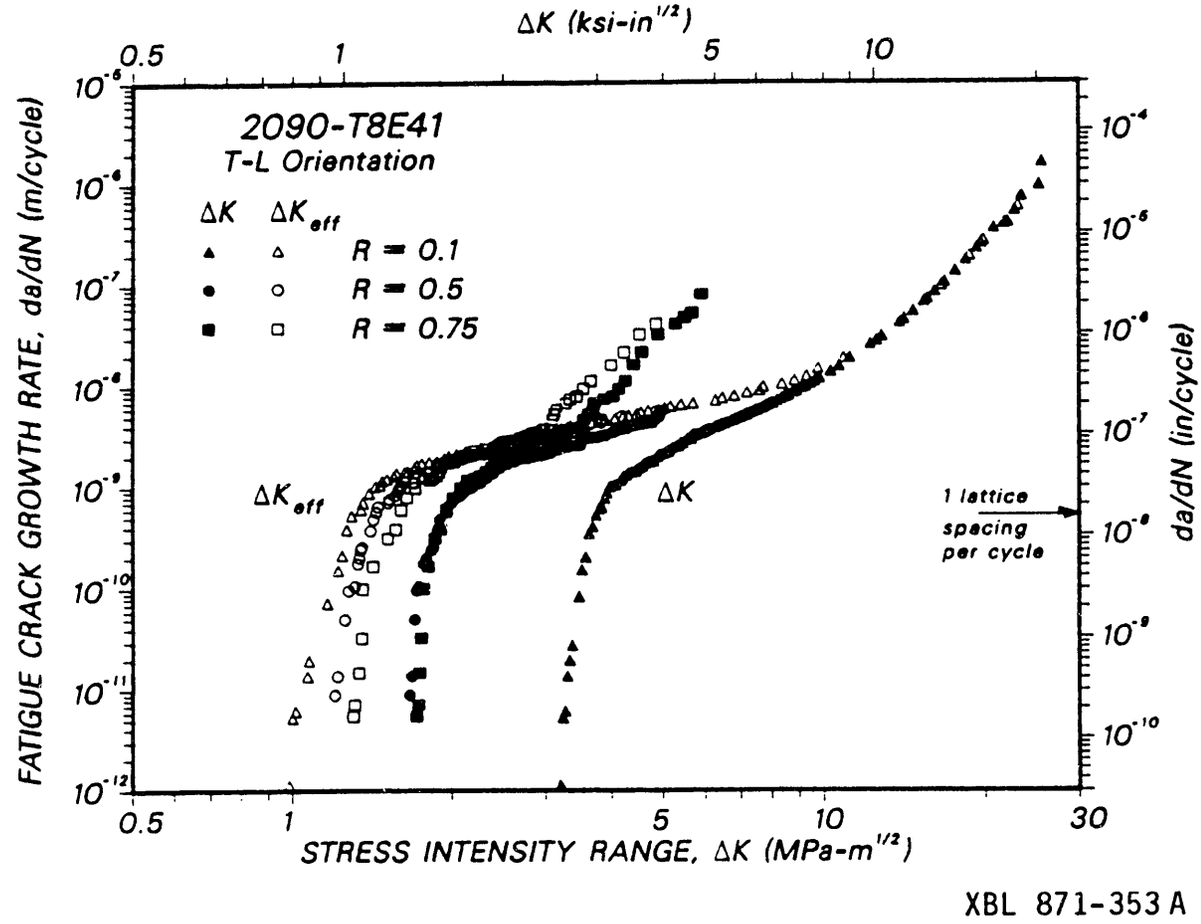

Fig. 11. Effect of load ratio R, on (long-crack) fatigue- crack propagation rates in 2090-T8E41 alloy, plotted as a function of both the nominal and effective stress-intensity ranges, ΔK and ΔK_{eff}, respectively.

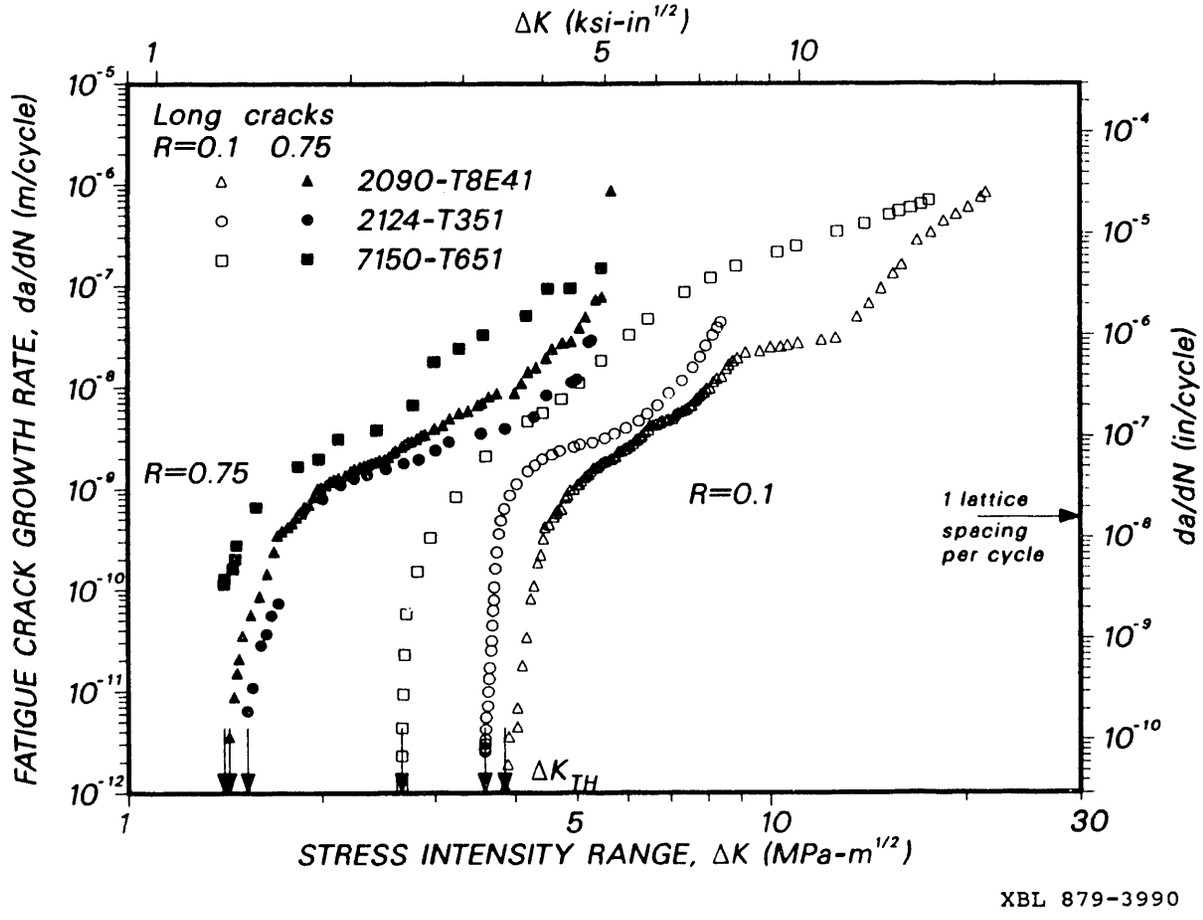

Fig. 12. Comparison of crack-growth rate behavior of long fatigue cracks in 2090-T8E41 with traditional 2124-T351 and 7150-T651 alloys, as a function of ΔK, at load ratios of 0.1 and 0.75. Note that the superior fatigue resistance of the Al-Li alloy at low load ratios is compromised at high load ratios where closure effects are minimized.

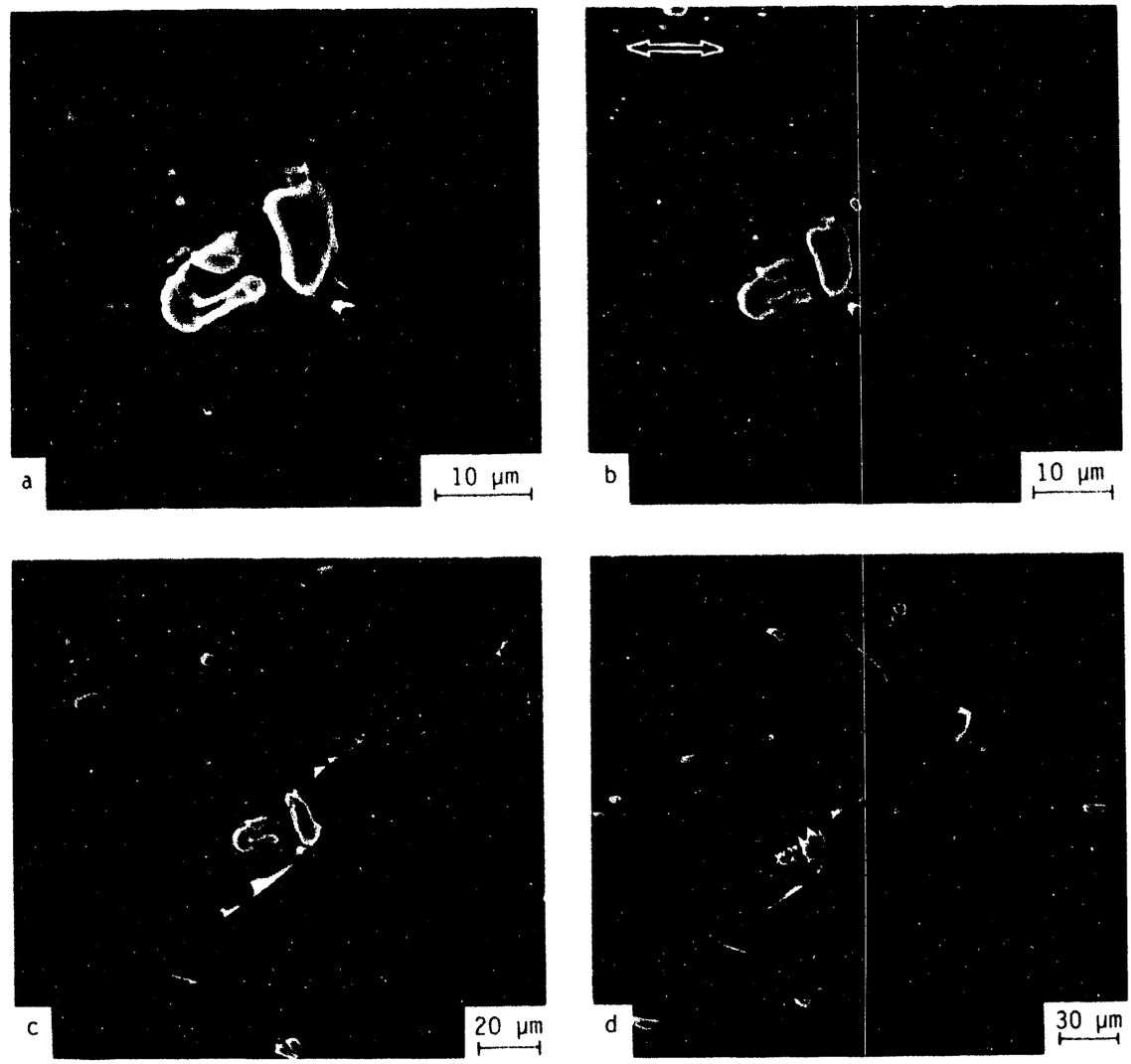

XBB 877-5508

Fig. 13. Growth morphology of microstructurally-small surface cracks initiated at intermetallic particles in 2091-T351 alloy, after cycling for a) 70,000, b) 80,000, c) 90,000 and d) 100,000 cycles. Scanning electron micrographs were obtained from gold coated cellulose-acetate replicas of the specimen surface. Horizontal arrow represents the direction of the loading.

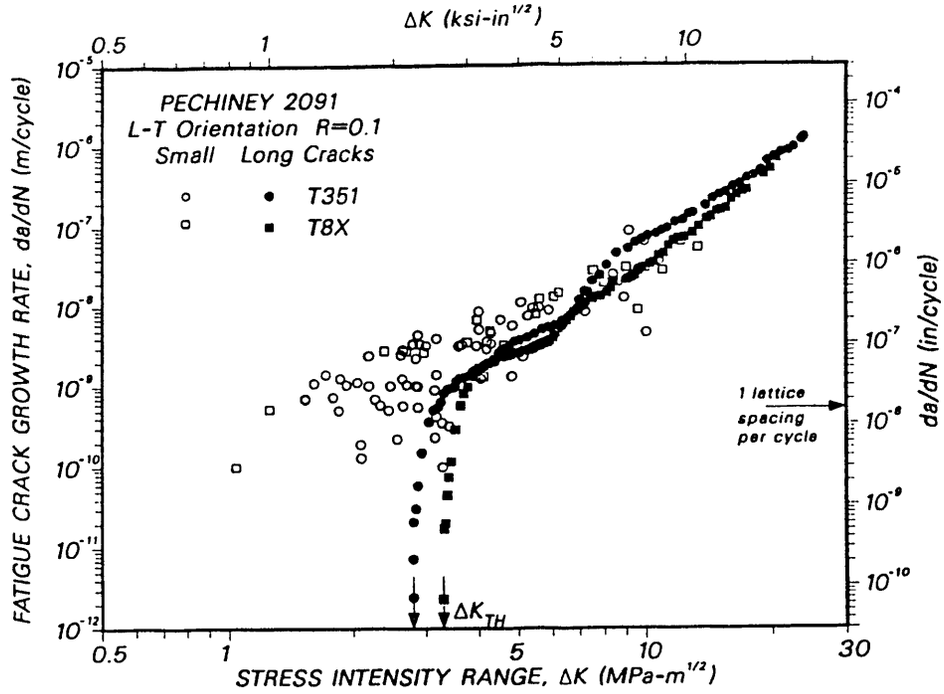

XBL 877-3199B
(top)

Fig. 14. Fatigue-crack growth behavior of long (> 10 mm) through-thickness and small (2-1000 μm) surface cracks in underaged (T351) and peak aged (T8X) 2091 alloy, showing small-crack growth rates some 2-3 orders of magnitude faster than long cracks at equivalent stress-intensity levels.

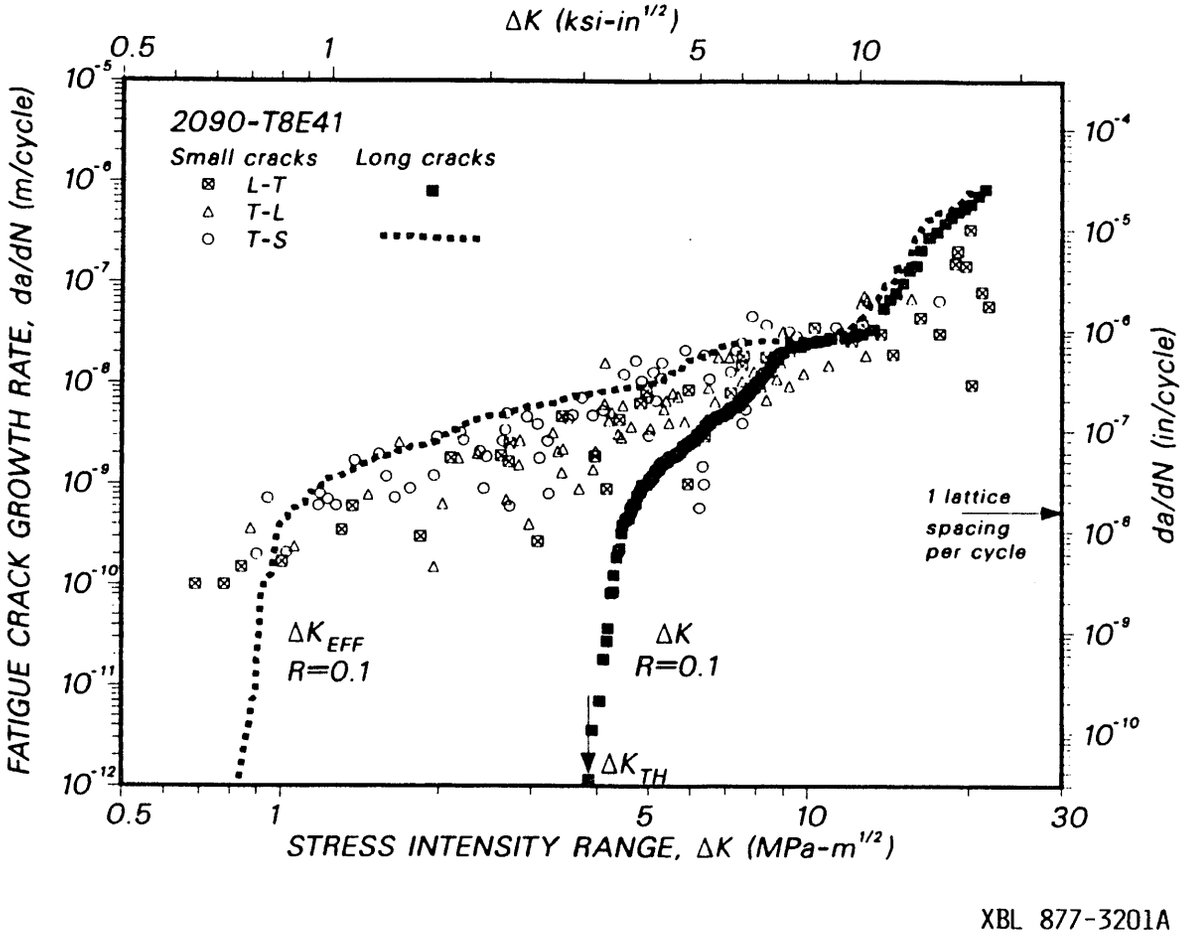

Fig. 15. Comparison of the growth-rate behavior of microstructurally-small (2-1000 μm) and long (> 10 mm) fatigue cracks in 2090-T8E41 alloy as a function of ΔK at R = 0.1. Note that when long- crack results are characterized in terms of ΔK_{eff} (dashed line), a closer correspondence is achieved between long- and small-crack data.

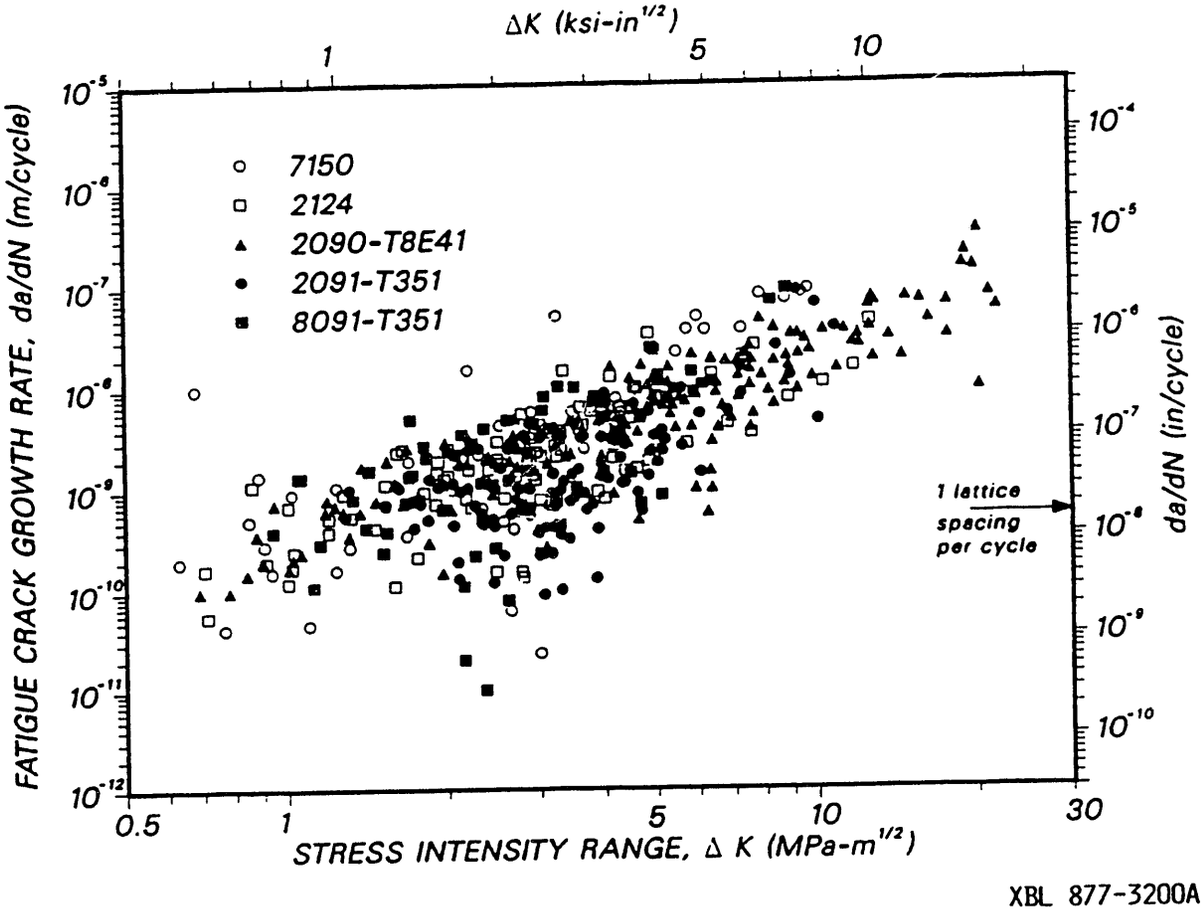

Fig. 16. Comparison of the growth-rate behavior, as a function of ΔK, of naturally-occurring, microstructurally-small surface cracks in commercial aluminum-lithium and traditional aluminum alloys, showing comparable small-crack growth resistance.

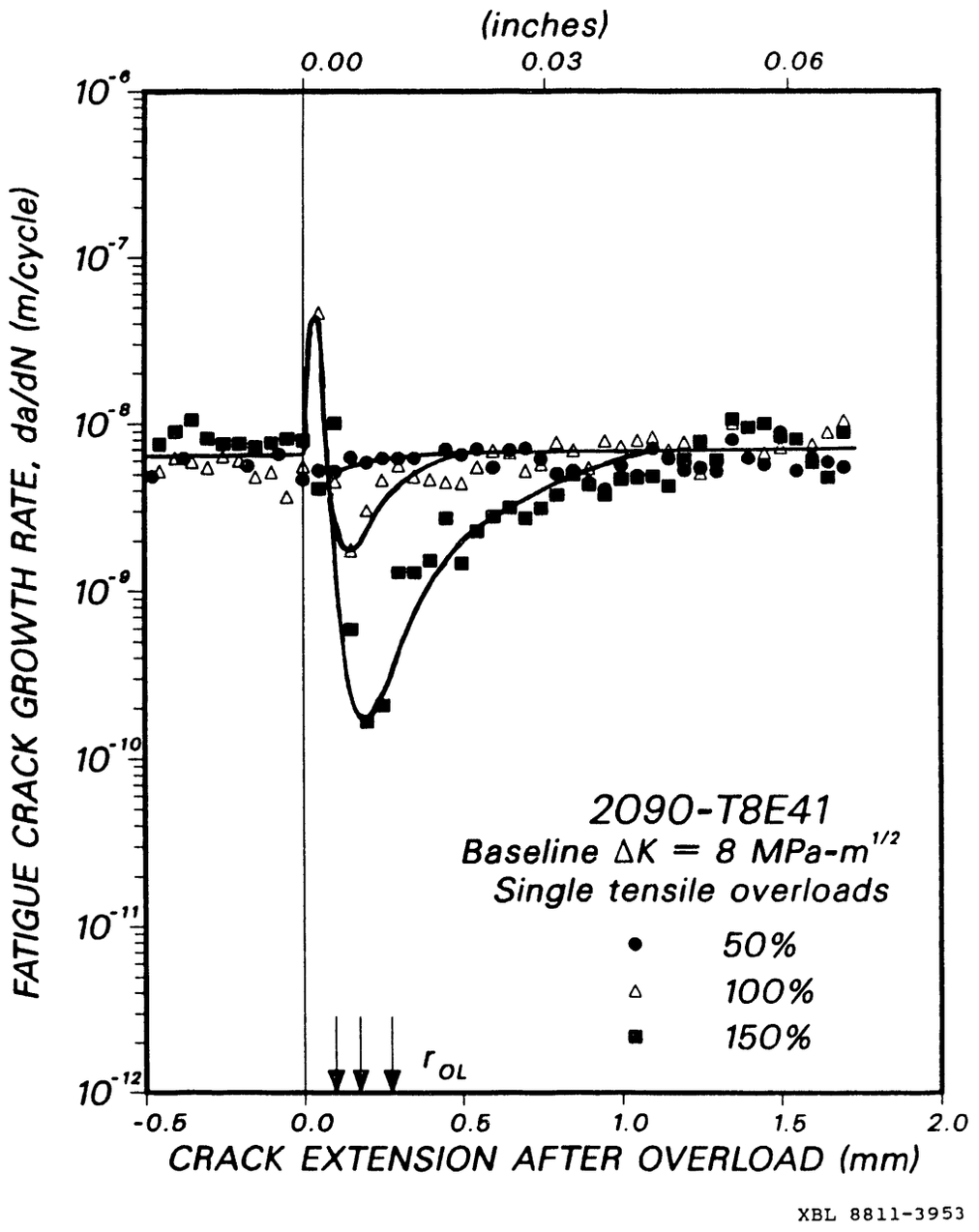

Fig. 17. Transient fatigue-crack growth rate behavior, as a function of crack extension, following 50, 100, 150% single tensile overloads in 2090-T8E41 alloy at a constant baseline ΔK of 8 MPa$\sqrt{m}$. Vertical arrows indicate computed maximum overload plastic-zone sizes, r_{oL}.

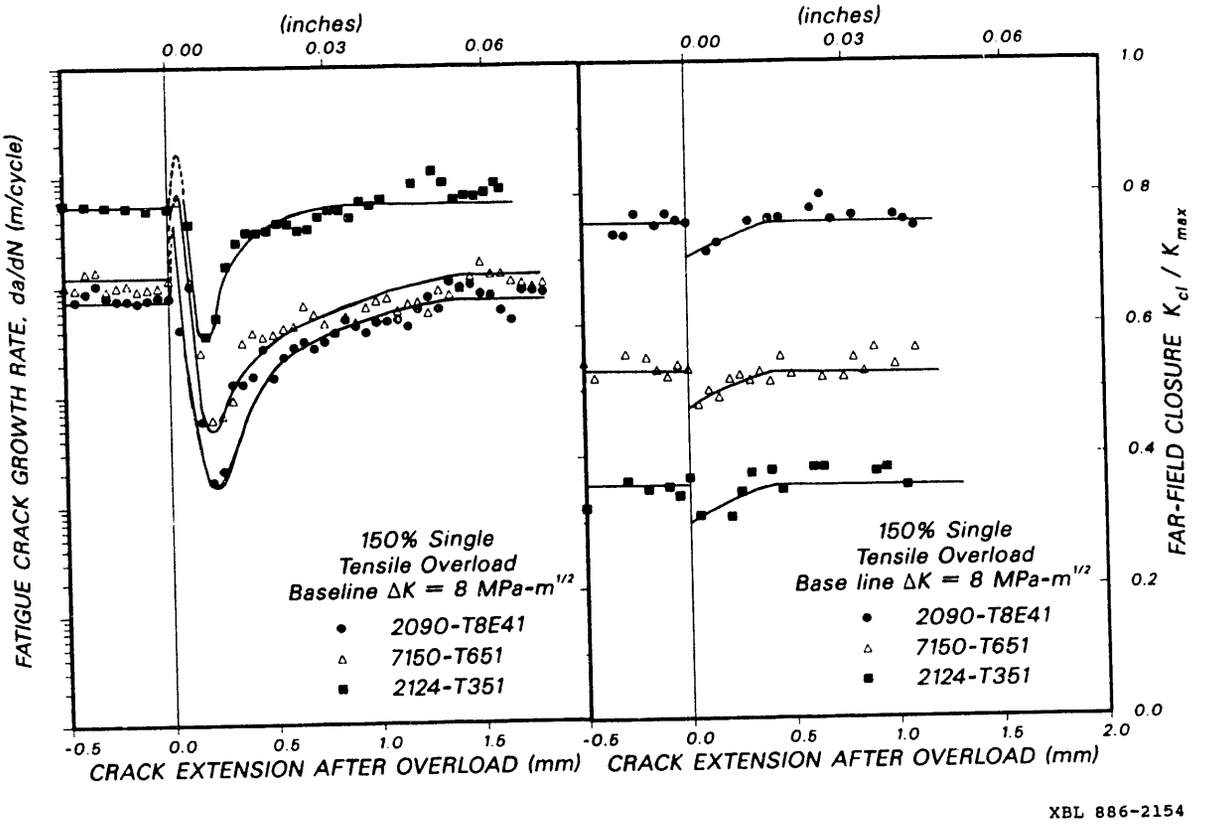

Fig. 18. Comparison of transient fatigue-crack growth behavior in 2090- T8E41 following 150% single tensile overloads, with behavior in 2124-T351 and 7150-T651, showing variation, as a function of crack extension, of a) crack-growth rates and b) far-field crack closure (K_{cl}/K_{max}). Note the greater delay in 2090, consistent with the higher levels of crack closure.

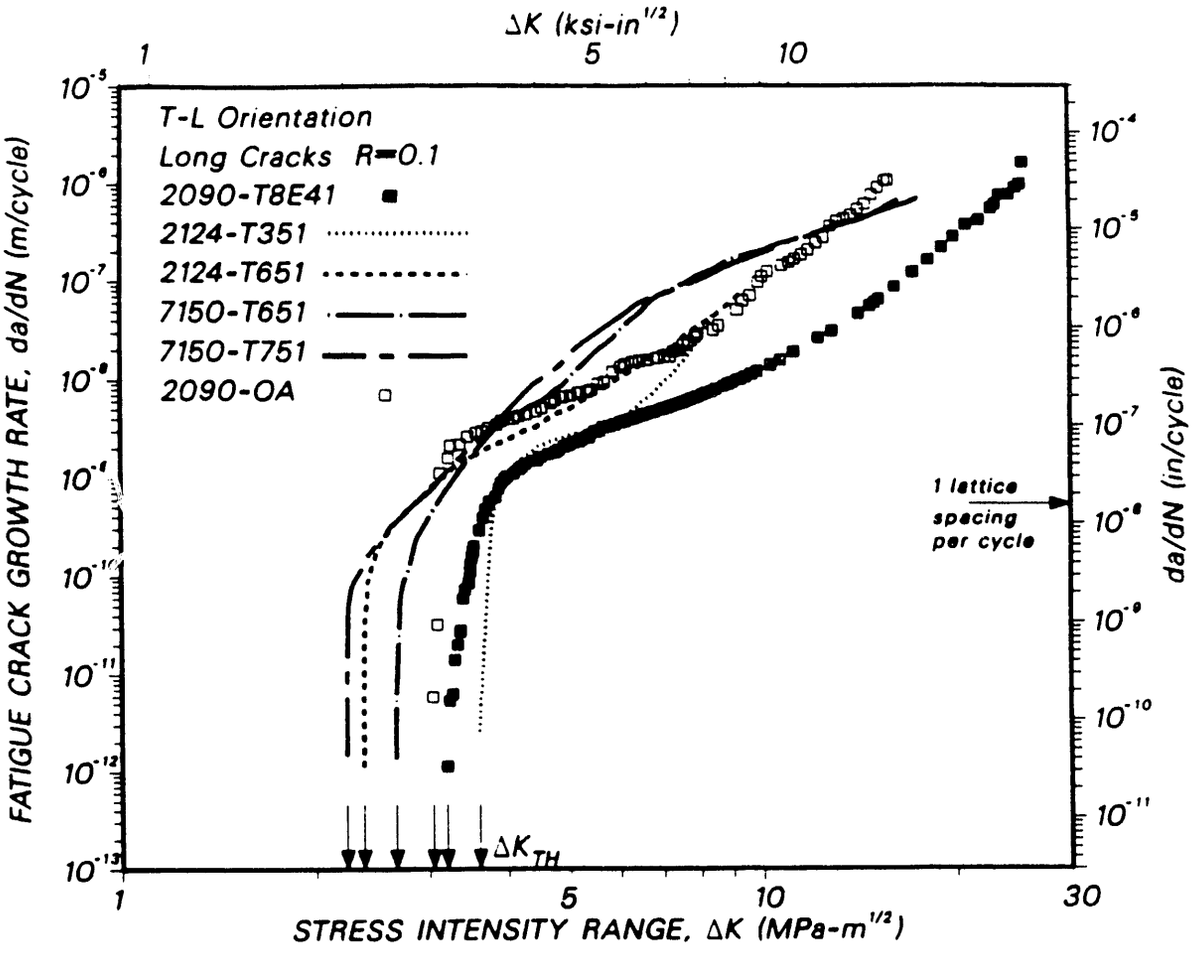

Fig. 19. Influence of high-temperature exposure of 1000 h at 163°C (overaging) on fatigue-crack propagation rates in alloy 2090-T8E41, compared with traditional aluminum alloys 2124 and 7150. Although overaging degrades the crack-growth resitance of the Al-Li alloy, it still remains comparable, if not superior, to the traditional alloys.

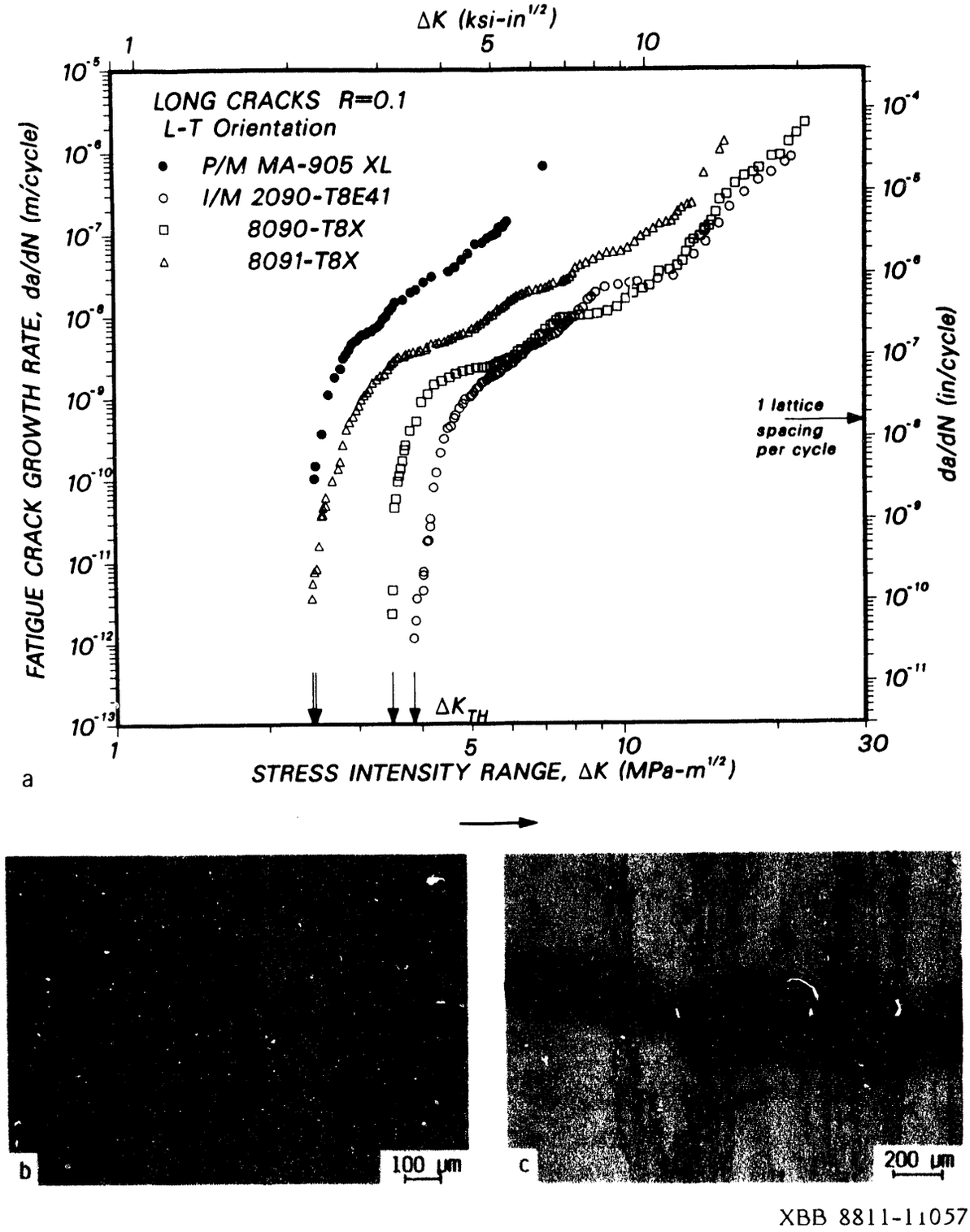

XBB 8811-11057

Fig. 20. Comparison of a) fatigue-crack growth rates and b,c) crack-path morphologies in fine-grained P/M mechanically alloyed Novamet Al-1.5Li-4Mg alloy (MA905-XL) with coarse-grained I/M 2090, 8090 and 8091 alloys (all T8 tempered). Note that growth rates are 1-2 orders of magnitude faster in the P/M alloy, consistent with a far more linear crack path and lower measured closure levels. Arrow indicates general direction of crack growth.

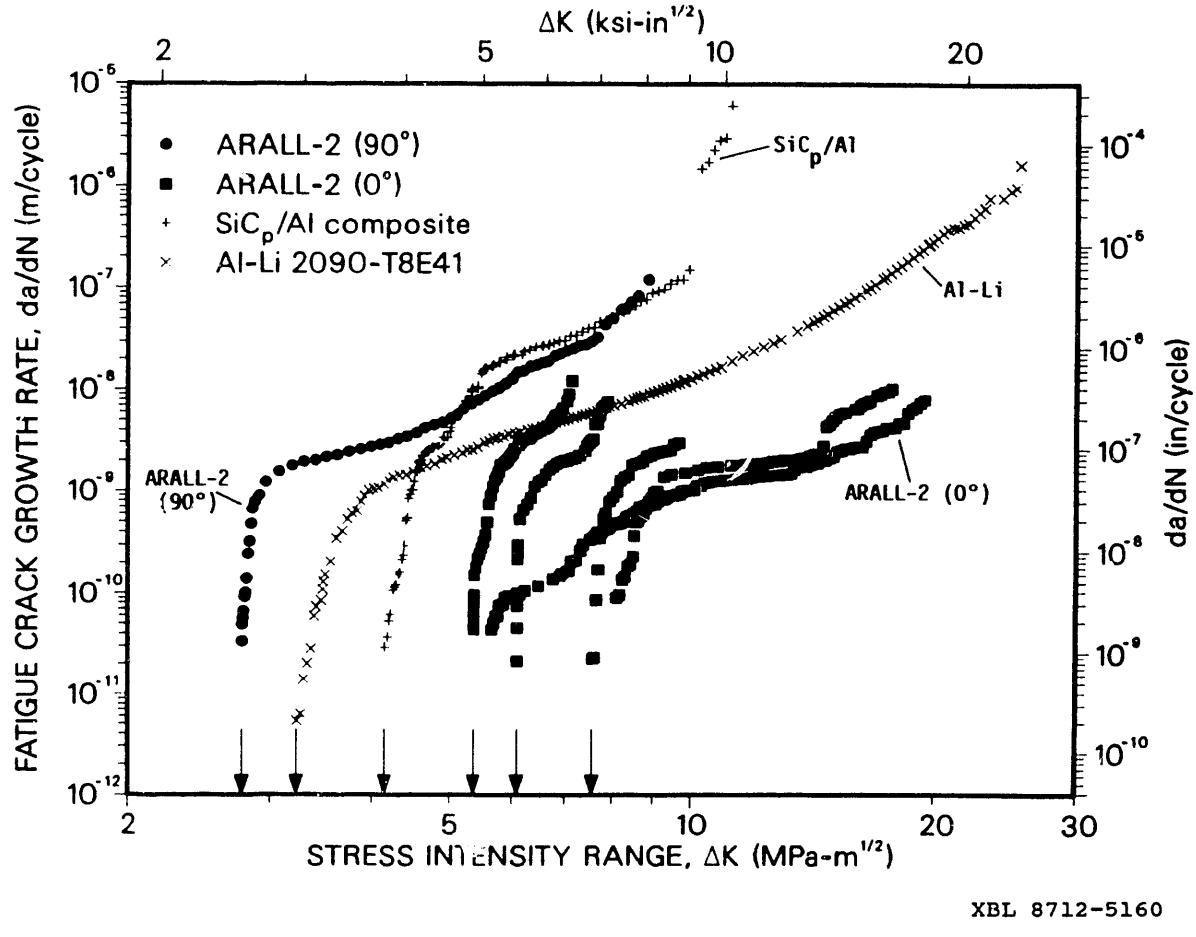

Fig. 21. Comparison of fatigue-crack growth resistance of advanced structural aerospace materials, namely aluminum-lithium alloys (2090-T8E41), metal-matrix composites (SiC-particulate reinforced 7091 P/M aluminum alloy) and ARALL-2 laminates. Data for ARALL and Al/SiC$_p$ composites are taken from the work of Ritchie *et al.* (1988) and Shang *et al.* (1988), respectively.

END

DATE
FILMED
11 122191